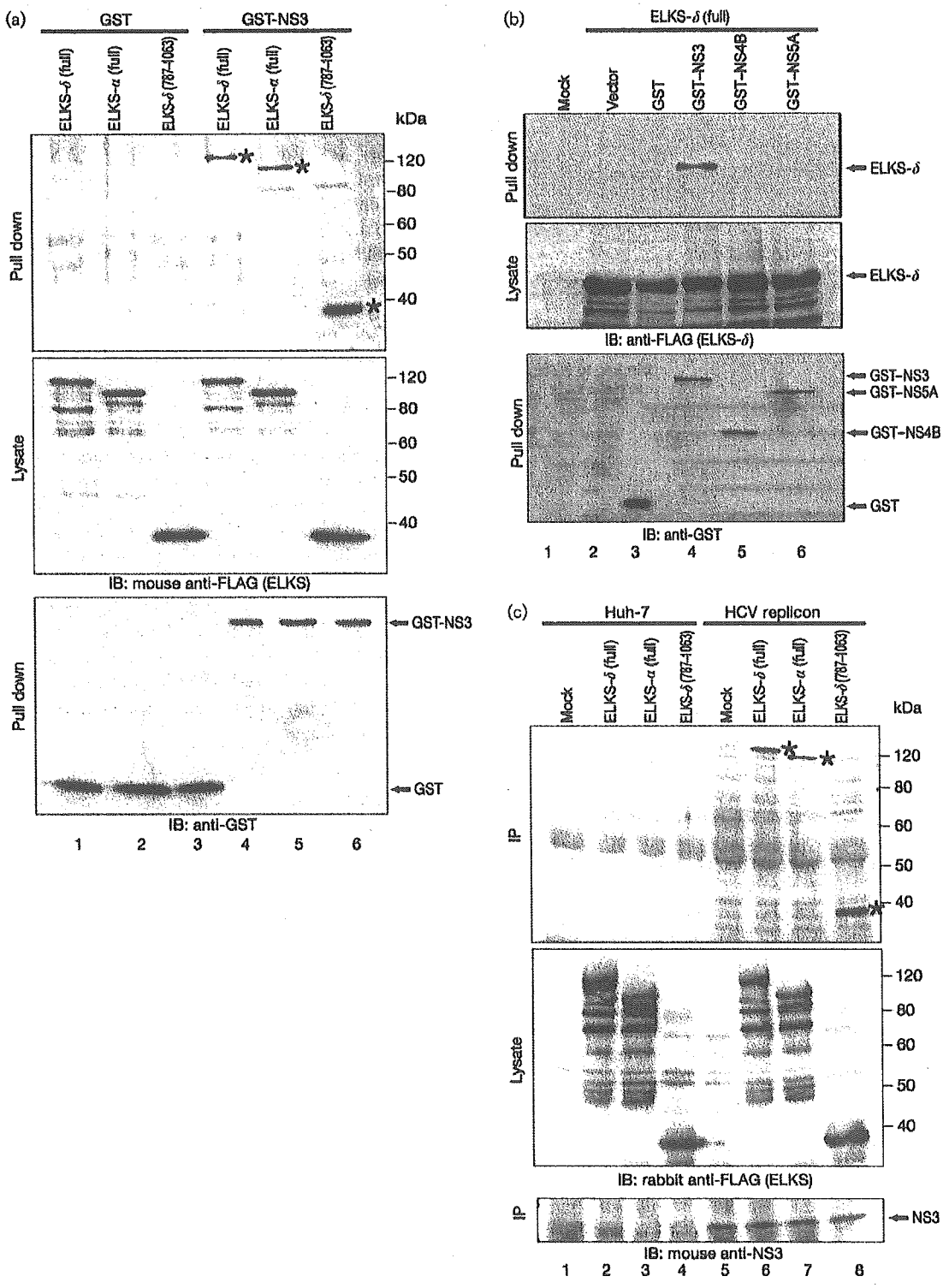

observed when ELKS-δ was expressed ectopically. Interestingly, the degree of interaction between NS3 and ELKS-δ correlated well with the level of increase in SEAP secretion (Fig. 7b). Moreover, SEAP secretion was enhanced in HCV RNA replicon-harbouring Huh-7 cells compared with HCV RNA-negative Huh-7 cells that had been cured by interferon treatment (Fig. 7c). These results strongly suggested that NS3 affects the cellular secretory pathway by interacting with ELKS-δ and ELKS-α.

Fig. 3. Full-length ELKS-δ and ELKS-α interact with full-length NS3 in cultured human cells. (a) FLAG-tagged full-length ELKS-δ (lanes 1 and 4), full-length ELKS-α (lanes 2 and 5) and a deletion mutant, ELKS-δ(787–1063) (lanes 3 and 6), were co-expressed in HeLa cells with GST (lanes 1–3) or full-length NS3 fused to GST (lanes 4–6). Cell lysates were pulled down with glutathione beads and probed with anti-FLAG antibody (upper panel). Lysates were directly (without being pulled down) probed with anti-FLAG antibody to confirm expression of ELKS-δ or ELKS-α (middle panel). Efficient pull-down was also verified (lower panel). (b) FLAG-tagged full-length ELKS-δ was co-expressed in HeLa cells with empty vector (lane 2), GST (lane 3), GST-tagged full-length NS3 (lane 4), full-length NS4B (lane 5) and full-length NS5A (lane 6). Cells lysates were pulled down by glutathione beads and probed with anti-FLAG antibody (upper panel). Lysates were directly probed with anti-FLAG antibody to confirm ELKS-δ expression (middle panel). Efficient pull down was also verified (lower panel). (c) FLAG-tagged full-length ELKS-δ (lanes 2 and 6), full-length ELKS-α (lanes 3 and 7) and a deletion mutant, ELKS-δ(787–1063) (lanes 4 and 8), were expressed in Huh-7 cells harbouring an HCV RNA replicon (lanes 5–8) or parental Huh-7 cells as a control (lanes 1–4). Cell lysates were immunoprecipitated with anti-NS3 polyclonal antibody and probed with anti-FLAG antibody (upper panel). Expression of ELKS-δ and ELKS-α (middle panel) and efficient immunoprecipitation of NS3 (lower panel) were also verified.

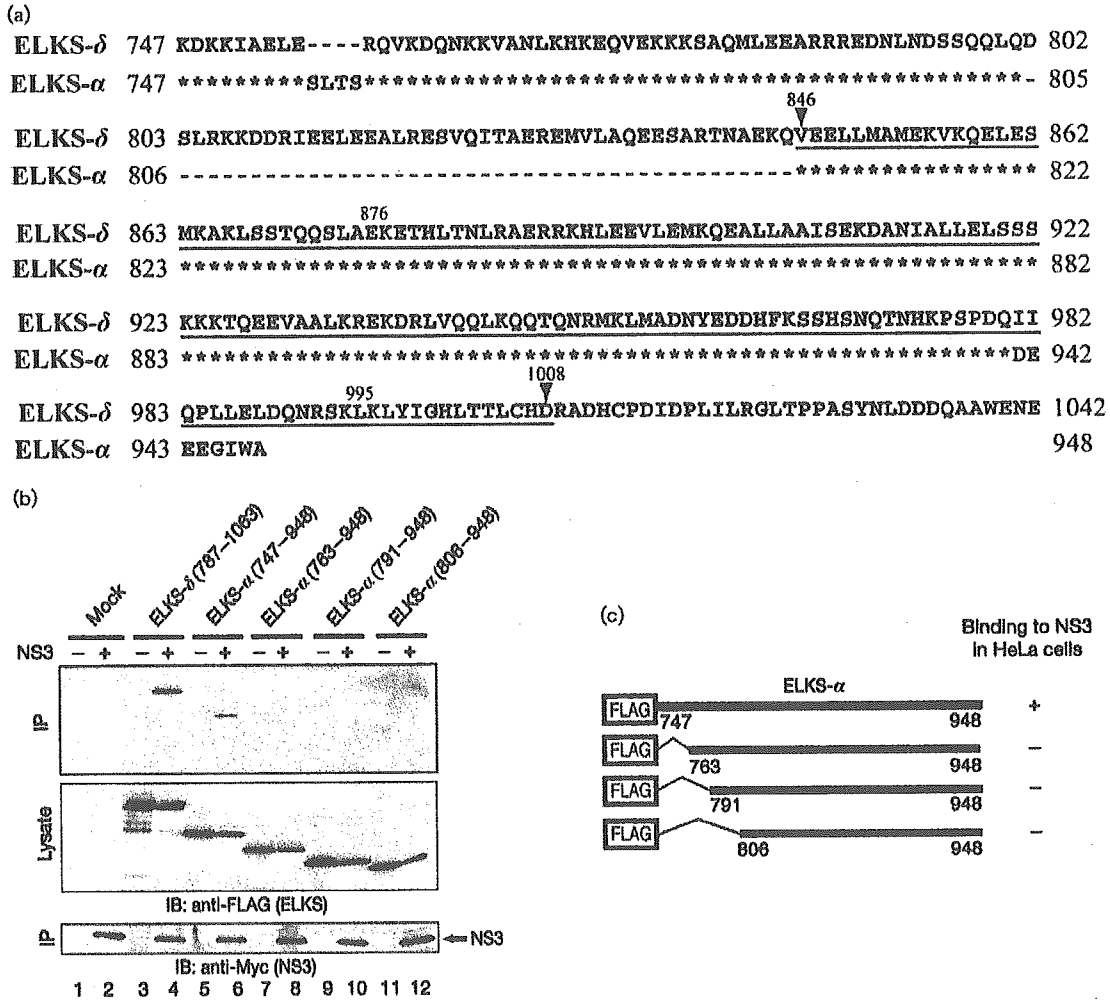

Fig. 4. Sequence comparison of C-terminal portions of ELKS-δ and ELKS-α. (a) Sequence alignment of a C-terminal portion of ELKS-δ and ELKS-α. Asterisks indicate identical residues. Hyphens indicate missing residues when compared with the other isoform. Underlined (aa 846–1008) is the minimum region of ELKS-δ required for interaction with NS3 (see Fig. 2). (b) A series of deletion mutants of FLAG-tagged ELKS-α was expressed without (odd-numbered lanes) or with (even-numbered lanes) Myc-tagged full-length NS3. ELKS-δ(787–1063) (lanes 3 and 4) served as a positive control. Cell lysates were immunoprecipitated using anti-Myc antibody and probed with anti-FLAG antibody (upper panel). Lysates were directly probed with anti-FLAG antibody to confirm expression of the ELKS-α mutants (middle panel). Efficient immunoprecipitation of NS3 was also verified (lower panel). (c) Schematic diagram of the ELKS-α deletion mutants. +, Moderate interaction [weaker than ELKS-δ(787–1063)]; –, no interaction.

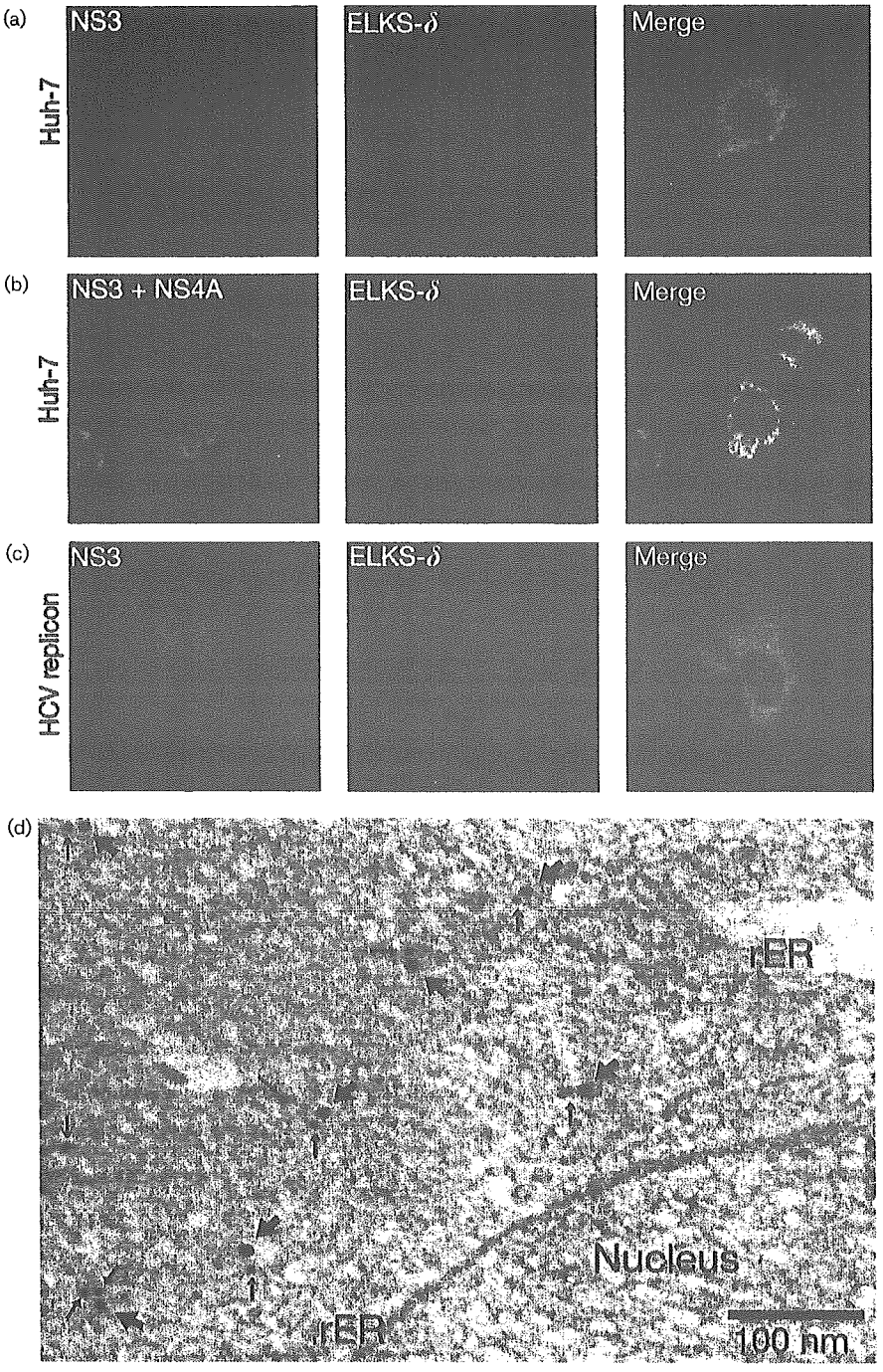

Fig. 5. Full-length ELKS-δ co-localizes with full-length NS3 in cultured human cells. FLAG-tagged full-length ELKS-δ was co-expressed in Huh-7 cells with Myc-tagged full-length NS3 in the absence (a) or presence (b) of NS4A, or in HCV RNA replicon-harbouring Huh-7 cells (c) and examined by double-staining immunofluorescence analysis. The orange colour in the cytoplasm observed in the merged pictures indicates co-localization of the two proteins. (d) FLAG-tagged full-length ELKS-δ was co-expressed with Myc-tagged full-length NS3 in HeLa cells. Cells were simultaneously stained with antibodies to Myc (5 nm diameter gold particles, thin arrows) and FLAG (10 nm diameter gold particles, thick arrows). Close proximity between both particles indicates tight interaction between the two proteins.

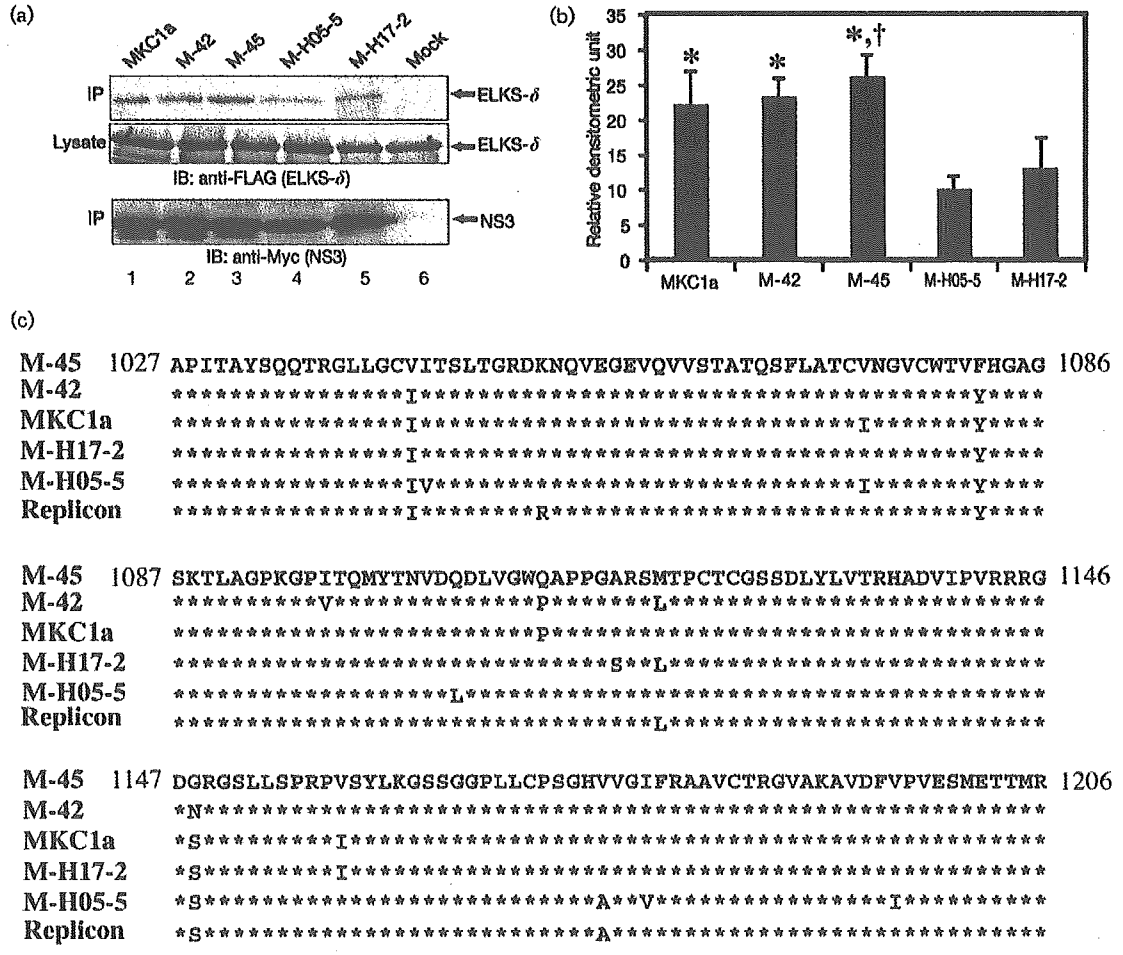

Fig. 6. NS3 interacts with ELKS-δ in a sequence-dependent manner. (a) FLAG-tagged full-length ELKS-δ was co-expressed with Myc-tagged full-length NS3 of different sequences by the plasmid-based expression method in HeLa cells. Cell lysates were immunoprecipitated using anti-Myc antibody and probed with anti-FLAG antibody (upper panel). Lysates were directly probed with anti-FLAG antibody to confirm ELKS-δ expression (middle panel). Efficient immunoprecipitation of NS3 was also verified (lower panel). (b) The intensities of the ELKS-δ bands that co-immunoprecipitated with NS3 were quantified using available software (tnimage-3.3.14) and normalized to ELKS-δ expression level. Results are shown as mean ± SD obtained from two independent experiments. *, $P<0{\cdot}05$, compared with M-H05-5; †, $P<0{\cdot}05$, compared with M-H17-2. (c) Sequence alignment of the N-terminal 180 residues of NS3 of different isolates. Asterisks indicate residues identical to those of M-45. The remaining C-terminal 451 residues were identical among the five isolates (see Methods).

DISCUSSION

In the present study, we demonstrated that an N-terminal protease domain of HCV NS3 interacts physically with ELKS-δ and ELKS-α in yeast and cultured human cells (Figs 1–5). This interaction was also observed in the presence of NS4A (Fig. 5b) and in HCV RNA replicon-harbouring cells (Figs 3c and 5c), where NS3 is expressed in the context of HCV RNA replication to form a virus replication complex in a unique membranous structure (Aizaki *et al.*, 2004). It was also demonstrated that the degree of interaction with ELKS-δ varied with different NS3 sequences (Fig. 6). The N-terminal 180 residues of M-42 and M-45, which bound to ELKS-δ more efficiently than M-H05-5, were derived from HCV isolates obtained from patients without HCC, whereas those of M-H05-5 and M-H17-2 were from patients with HCC (Ogata *et al.*, 2002, 2003). It is intriguing to speculate that certain NS3 sequences with reduced ELKS-δ binding are more likely to interact with, and modulate the function of, another host factor(s), such as p53 (L. Deng and others, unpublished data; Ishido & Hotta, 1998; Muramatsu *et al.*, 1997), thus facilitating the development of HCC. However, with the limited number of samples tested, it was difficult to draw a conclusion about the correlation between the NS3–ELKS-δ interaction and certain clinical symptoms, including HCC.

ELKS was initially identified as a protein fused to the RET

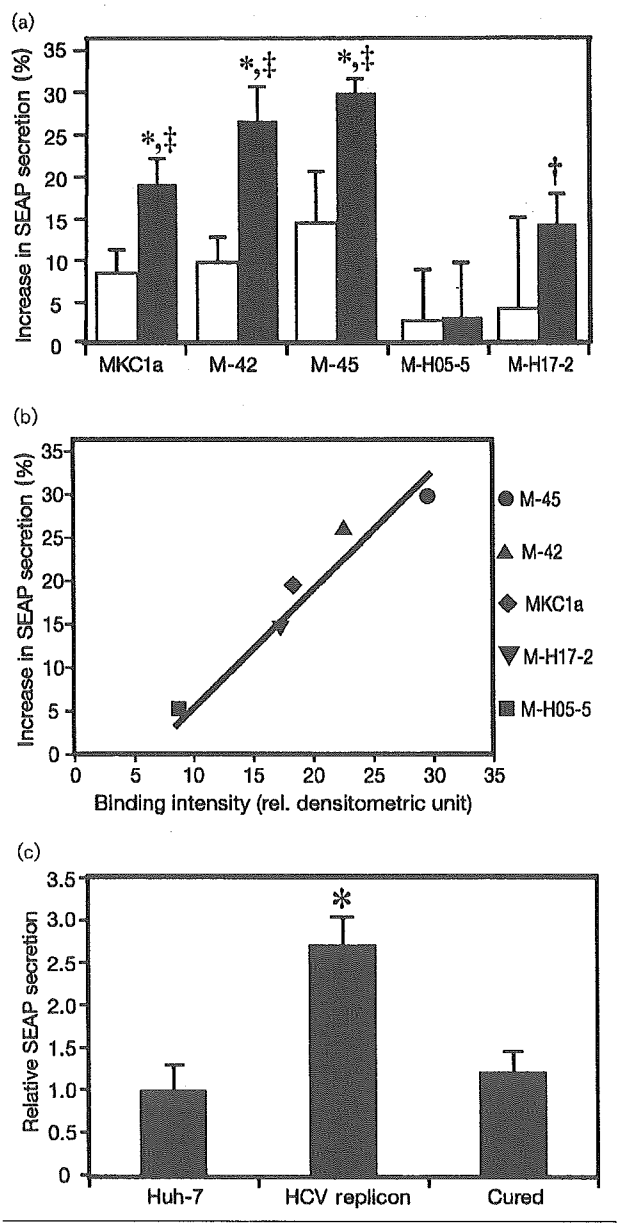

Fig. 7. NS3 enhances SEAP secretion from cells in a sequence-dependent manner. (a) Myc-tagged full-length NS3 proteins of different sequences were co-expressed with SEAP (pSEAP2-Control) and *Renilla* luciferase (pRL-SV40) in HeLa cells, in the absence (open columns) or presence (filled columns) of ectopic, full-length ELKS-δ. An irrelevant protein (GST) served as a control for NS3. SEAP activity in the medium was measured and normalized to *Renilla* luciferase activities. The percentage increase in NS3-mediated SEAP secretion over the control is shown. Results are given as the mean ± SD from three independent experiments. *, $P<0{\cdot}001$; †, $P<0{\cdot}01$, compared with the control; ‡, $P<0{\cdot}05$, compared with the value in the absence of ectopic ELKS-δ expression (open column). (b) Correlation between NS3-mediated enhancement of SEAP secretion (percentage increase) and the degree of interaction with ELKS-δ. Correlation coefficient (r) = 0·97973485 ($P<0{\cdot}0001$). (c) Parental Huh-7 cells, HCV RNA replicon-harbouring Huh-7 cells and HCV RNA-negative cured Huh-7 cells were co-transfected with pSEAP2-Control and pRL-SV40. SEAP activity in the medium was measured and normalized to *Renilla* luciferase activities. Results are given as the mean ± SD of the relative SEAP secretion compared with the parental Huh-7. *, $P<0{\cdot}05$, compared with parental and cured Huh-7 cells.

proto-oncogene product in human papillary thyroid carcinoma (Nakata *et al.*, 1999). Four other splice variants of the ELKS protein family were subsequently identified and designated ELKS-β, -γ, -δ and -ε, with the prototype isoform being renamed ELKS-α (Nakata *et al.*, 2002). A number of related proteins highly homologous to the ELKS proteins were identified in rat, named CAST (CAST1, CAST2α and CAST2β; Deguchi-Tawarada *et al.*, 2004; Ohtsuka *et al.*, 2002) and ERC (ERC1a, ERC1b and ERC2; Wang *et al.*, 2002). Another research group discovered two related mouse proteins that interacted specifically with a small GTPase protein, Rab6, and therefore the proteins were named Rab6IP2A and Rab6IP2B (Monier *et al.*, 2002). Sequence alignment has revealed that ELKS, CAST, ERC and Rab6IP2 are orthologous members of the same protein family in human, rat and mouse. Their expression profiles in the body differ with different isoforms, with ELKS-α, CAST2α, Rab6IP2A, ERC1b and ERC2 expressed only in the brain, while ELKS-δ, Rab6IP2B and ERC1a are expressed ubiquitously outside of the brain (Nakata *et al.*, 2002; Deguchi-Tawarada *et al.*, 2004). In the present study, we mapped the minimum NS3-binding sequences to the regions spanning aa 846–1008 of ELKS-δ (Fig. 2) and aa 747–948 of ELKS-α (Fig. 4). Since the sequence of ELKS-δ from aa 846 to 1008 completely matches that of the corresponding region of ELKS-ε (aa 874–1036), ELKS-ε is most likely to interact with NS3. On the other hand, when compared with the minimum NS3-binding sequence of ELKS-α (aa 747–948), the corresponding region of ELKS-β (aa 747–992) and ELKS-γ (aa 475–720) have an identical insertion of 44 residues between positions 805 and 806 of ELKS-α. At present, we do not know whether or not this insertion affects the interaction with NS3.

Rab6IP2A and Rab6IP2B have been reported partially to inhibit the endosome-to-Golgi retrograde transport pathway through their binding to Rab6 (Monier *et al.*, 2002). Similarly, CAST and ERC proteins have been postulated to modulate neurotransmitter release through interaction with Rab3A-interacting molecules that are localized in the pre-synaptic active zone and involved in exocytosis of neurotransmitters in a Rab3-dependent manner (Deguchi-Tawarada *et al.*, 2004; Ohtsuka *et al.*, 2002; Wang *et al.*, 2002). It is thus possible that certain ELKS-binding proteins, including viral products, affect intracellular transport and secretory pathways, either positively or negatively, by counteracting or augmenting the function of ELKS proteins. Indeed, we observed that HCV NS3 enhanced SEAP

secretion from cells. Interestingly, the degree of enhancement of secretion correlated well with the degree of binding between NS3 and ELKS-δ (Fig. 7b). It has been reported that Rab6 is expressed in hepatocytes, playing an important role in regulating intracellular transport at the level of the Golgi complex (Feldmann *et al.*, 1995). In addition, ELKS-δ and its mouse counterpart Rab6IP2B are expressed ubiquitously in the body (Monier *et al.*, 2002; Nakata *et al.*, 2002). Therefore, it is reasonable to assume that, even in a natural setting, i.e. in HCV-infected hepatocytes *in vivo*, NS3 interacts with ELKS-δ to modulate Rab6-dependent intracellular transport and secretory pathways, thereby facilitating intracellular transport of viral components so that virion formation takes place efficiently. However, the precise role of this interaction in the virus life cycle and/or viral pathogenesis is still unknown and awaits further investigation.

We observed enhanced SEAP secretion from Huh-7 cells harbouring an HCV subgenomic RNA replicon, compared with secretion from parental Huh-7 cells and interferon-treated cured cells (Fig. 7c). In this context, it was recently reported that the rate of MHC class I traffic to the cell surface was inhibited in Huh-7 cells harbouring an HCV subgenomic RNA replicon and that the inhibition was probably mediated by the NS4A/B precursor protein (Konan *et al.*, 2003). At present, we do not know the reason for the apparent discrepancy between their results (inhibited MHC class I traffic) and ours (enhanced SEAP secretion) in HCV RNA replicon-harbouring cells. It is possible that these events occur through different mechanisms, which selectively modulate intracellular transport and secretion of a particular protein(s).

Recently, Ducut Sigala *et al.* (2004) identified ELKS-α as an essential regulatory subunit of the IκB kinase complex, a modulator of nuclear factor-κB (NF-κB) transcription factor activation. They showed that ELKS-α was involved in induced expression of NF-κB target genes, including pro-inflammatory genes, and also in establishing a cellular anti-apoptotic status in response to tumour necrosis factor-α. These findings, together with our present observations, imply that NS3, through its interaction with ELKS-δ and ELKS-α, may modulate NF-κB activation, thereby facilitating HCV pathogenesis, such as inflammation and tumour formation in the liver. Further studies are needed to elucidate these issues.

ACKNOWLEDGEMENTS

The authors are grateful to Dr M. Emi (Institute of Gerontology, Nippon Medical School, Kawasaki, Kanagawa, Japan) for providing the plasmids pDR2-ELKS-δ (p14) and pDR2-ELKS-α (p32). Thanks are also due to Dr R. Bartenschlager (University of Heidelberg, Heidelberg, Germany) for providing an HCV subgenomic RNA replicon (pFK5B2884Gly). This work was supported in part by grants-in-aid for Scientific Research from the Ministry of Education, Culture, Sports, Science and Technology, Japan, and the Japan Society for the Promotion of Science.

REFERENCES

Aizaki, H., Lee, K.-J., Sung, V. M.-H., Ishiko, H. & Lai, M. M. C. (2004). Characterization of the hepatitis C virus RNA replication complex associated with lipid rafts. *Virology* **324**, 450–461.

Aoubala, M., Holt, J., Clegg, R. A., Rowlands, D. J. & Harris, M. (2001). The inhibition of cAMP-dependent protein kinase by full-length hepatitis C virus NS3/4A complex is due to ATP hydrolysis. *J Gen Virol* **82**, 1637–1646.

Borowski, P., Heiland, M., Feucht, H. & Laufs, R. (1999a). Characterisation of non-structural protein 3 of hepatitis C virus as modulator of protein phosphorylation mediated by PKA and PKC: evidences for action on the level of substrate and enzyme. *Arch Virol* **144**, 687–701.

Borowski, P., Schulze zur Wiesch, J., Resch, K., Feucht, H., Laufs, R. & Schmitz, H. (1999b). Protein kinase C recognizes the protein kinase A-binding motif of nonstructural protein 3 of hepatitis C virus. *J Biol Chem* **274**, 30722–30728.

Borowski, P., Kühl, R., Laufs, R., Schulze zur Wiesch, J. & Heiland, M. (1999c). Identification and characterization of a histone binding site of the non-structural protein 3 of hepatitis C virus. *J Clin Virol* **13**, 61–69.

Choo, Q. L., Kuo, G., Weiner, A. J., Overby, L. R., Bradley, D. W. & Houghton, M. (1989). Isolation of a cDNA clone derived from a blood-borne non-A, non-B viral hepatitis genome. *Science* **244**, 359–362.

Cullen, B. R. & Malim, M. H. (1992). Secreted placental alkaline phosphatase as a eukaryotic reporter gene. *Methods Enzymol* **216**, 362–368.

Deguchi-Tawarada, M., Inoue, E., Takao-Rikitsu, E., Inoue, M., Ohtsuka, T. & Takai, Y. (2004). CAST2: identification and characterization of a protein structurally related to the presynaptic cytomatrix CAST. *Genes Cells* **9**, 15–23.

Ducut Sigala, J. L., Bottero, V., Young, D. B., Shevchenko, A., Mercurio, F. & Verma, I. M. (2004). Activation of transcription factor NF-κB requires ELKS, and IκB kinase regulatory subunit. *Science* **304**, 1963–1967.

Echard, A., Opdam, F. J., de Leeuw, H. J., Jollivet, F., Savelkoul, P., Hendriks, W., Voorberg, J., Goud, B. & Fransen, J. A. (2000). Alternative splicing of the human Rab6A gene generates two close but functionally different isoforms. *Mol Biol Cell* **11**, 3819–3833.

Feldmann, G., Durand-Schneider, A. M. & Goud, B. (1995). Behaviour of the small GTP-binding protein rab6 in the liver of normal rats and rats presenting an acute inflammatory reaction. *Biol Cell* **83**, 121–125.

He, Q.-Q., Cheng, R.-X., Sun, Y., Feng, D.-Y., Chen, Z.-C. & Zeng, H. (2003). Hepatocyte transformation and tumor development induced by hepatitis C virus NS3 C-terminal deleted protein. *World J Gastroenterol* **9**, 474–478.

Hijikata, M., Kato, N., Ootsuyama, Y., Nakagawa, M. & Shimotohno, K. (1991). Gene mapping of the putative structural region of the hepatitis C virus genome by in vitro processing analysis. *Proc Natl Acad Sci U S A* **88**, 5547–5551.

Hijikata, M., Mizushima, H., Tanji, Y., Komoda, Y., Hirowatari, Y., Akagi, T., Kato, N., Kimura, K. & Shimotohno, K. (1993). Proteolytic processing and membrane association of putative nonstructural proteins of hepatitis C virus. *Proc Natl Acad Sci U S A* **90**, 10773–10777.

Ishido, S. & Hotta, H. (1998). Complex formation of the nonstructural protein 3 of hepatitis C virus with the p53 tumor suppressor. *FEBS Lett* **438**, 258–262.

Iwai, A., Hasumura, Y., Nojima, T. & Takegami, T. (2003). Hepatitis C virus nonstructural protein NS3 binds to Sm-D1, a small nuclear ribonucleoprotein associated with autoimmune disease. *Microbiol Immunol* **47**, 601–611.

Khu, Y.-L., Tan, Y.-J., Lim, S.-G., Hong, W. & Goh, P.-Y. (2004). Hepatitis C virus non-structural protein NS3 interacts with LMP7, a component of the immunoproteasome, and affects its proteasome activity. *Biochem J* **384**, 401–409.

Konan, K. V., Giddings, T. H., Jr, Ikeda, M., Li, K., Lemon, S. M. & Kirkegaard, K. (2003). Nonstructural protein precursor NS4A/B from hepatitis C virus alters function and ultrastructure of host secretory apparatus. *J Virol* **77**, 7843–7855.

Lohmann, V., Körner, F., Dobierzewska, A. & Bartenschlager, R. (2001). Mutations in hepatitis C virus RNAs conferring cell culture adaptation. *J Virol* **75**, 1437–1449.

Martinez, O., Schmidt, A., Salamero, J., Hoflack, B., Roa, M. & Goud, B. (1994). The small GTP-binding protein rab6 functions in intra-Golgi transport. *J Cell Biol* **127**, 1575–1588.

Monier, S., Jollivet, F., Janoueix-Lerosey, I., Johannes, L. & Goud, B. (2002). Characterization of novel Rab6-interacting proteins involved in endosome-to-TGN transport. *Traffic* **3**, 289–297.

Muramatsu, S., Ishido, S., Fujita, T., Itoh, M. & Hotta, H. (1997). Nuclear localization of the NS3 protein of hepatitis C virus and factors affecting the localization. *J Virol* **71**, 4954–4961.

Nakata, T., Kitamura, Y., Shimizu, K., Tanaka, S., Fujimori, M., Yokoyama, S., Ito, K. & Emi, M. (1999). Fusion of a novel gene, *ELKS*, to *RET* due to translocation t(10;12)(q11;p13) in a papillary thyroid carcinoma. *Genes Chromosomes Cancer* **25**, 97–103.

Nakata, T., Yokota, T., Emi, M. & Minami, S. (2002). Differential expression of multiple isoforms of the *ELKS* mRNAs involved in a papillary thyroid carcinoma. *Genes Chromosomes Cancer* **35**, 30–37.

Ogata, S., Ku, Y., Yoon, S., Makino, S., Nagano-Fujii, M. & Hotta, H. (2002). Correlation between secondary structure of an amino-terminal portion of the nonstructural protein 3 (NS3) of hepatitis C virus and development of hepatocellular carcinoma. *Microbiol Immunol* **46**, 549–554.

Ogata, S., Florese, R. H., Nagano-Fujii, M. & 7 other authors (2003). Identification of hepatitis C virus (HCV) subtype 1b strains that are highly, or only weakly, associated with hepatocellular carcinoma on the basis of the secondary structure of an amino-terminal portion of the HCV NS3 protein. *J Clin Microbiol* **41**, 2835–2841.

Ohtsuka, T., Takao-Rikitsu, E., Inoue, E. & 8 other authors (2002). CAST: a novel protein of the cytomatrix at the active zone of synapses that forms a ternary complex with RIM1 and Munc13-1. *J Cell Biol* **158**, 577–590.

Reed, K. E. & Rice, C. M. (2000). Overview of hepatitis C virus genome structure, polyprotein processing, and protein properties. *Curr Top Microbiol Immunol* **242**, 55–84.

Rho, J., Choi, S., Seong, Y. R., Choi, J. & Im, D.-S. (2001). The arginine-1493 residue in QRRGRTGR1493G motif IV of the hepatitis C virus NS3 helicase domain is essential for NS3 protein methylation by the protein arginine methyltransferase 1. *J Virol* **75**, 8031–8044.

Sakamuro, D., Furukawa, T. & Takegami, T. (1995). Hepatitis C virus nonstructural protein NS3 transforms NIH 3T3 cells. *J Virol* **69**, 3893–3896.

Taguchi, T., Nagano-Fujii, M., Akutsu, M., Kadoya, H., Ohgimoto, S., Ishido, S. & Hotta, H. (2004). Hepatitis C virus NS5A protein interacts with 2′,5′-oligoadenylate synthetase and inhibits antiviral activity of IFN in an IFN sensitivity-determining region-independent manner. *J Gen Virol* **85**, 959–969.

Takigawa, Y., Nagano-Fujii, M., Deng, L., Hidajat, R., Tanaka, M., Mizuta, H. & Hotta, H. (2004). Suppression of hepatitis C virus replicon by RNA interference directed against the NS3 and NS5B regions of the viral genome. *Microbiol Immunol* **48**, 591–598.

Tellinghuisen, T. L. & Rice, C. M. (2002). Interaction between hepatitis C virus proteins and host cell factors. *Curr Opin Microbiol* **5**, 419–427.

Tong, W.-Y., Nagano-Fujii, M., Hidajat, R., Deng, L., Takigawa, Y. & Hotta, H. (2002). Physical interaction between hepatitis C virus NS4B protein and CREB-RP/ATF6*β*. *Biochem Biophys Res Commun* **299**, 366–372.

Wang, Y., Liu, X., Biederer, T. & Südhof, T. C. (2002). A family of RIM-binding proteins regulated by alternative splicing: implications for the genesis of synaptic active zones. *Proc Natl Acad Sci U S A* **99**, 14464–14469.

WHO (1999). Hepatitis C – global prevalence (update). *Wkly Epidemiol Rec* **74**, 425–427.

Wölk, B., Sansonno, D., Kräusslich, H. G., Dammacco, F., Rice, C. M., Blum, H. E. & Moradpour, D. (2000). Subcellular locacalization, stability, and *trans*-cleavage competence of the hepatitis C virus NS3–NS4A complex expressed in tetracycline-regulated cell lines. *J Virol* **74**, 2293–2304.

Zemel, R., Gerechet, S., Greif, H. & 7 other authors (2001). Cell transformation induced by hepatitis C virus NS3 serine protease. *J Viral Hepat* **8**, 96–102.

Microbiol. Immunol., 49(3), 265–273, 2005

Editor-Communicated Paper

Nonstructural Proteins 4A and 4B of Hepatitis C Virus Transactivate the Interleukin 8 Promoter

Hiroyasu Kadoya[1,2], Motoko Nagano-Fujii[1], Lin Deng[1], Naoki Nakazono[2], and Hak Hotta*[,1]

[1]*Division of Microbiology, Kobe University Graduate School of Medicine, Kobe, Hyogo 650–0017, Japan, and* [2]*Division of Environmental Health, Epidemiology and Infectious Diseases, Kobe University Graduate School of Medicine, Kobe, Hyogo 654–0142, Japan*

Communicated by Dr. Nobuyuki Kato: Received December 28, 2004. Accepted January 4, 2005

***Abstract*: Interleukin 8 (IL-8) is induced in many cell types by various stimuli including virus infection. It was reported that nonstructural protein 5A (NS5A) of hepatitis C virus (HCV) was involved in induction of IL-8 expression at both mRNA and protein levels in cultured human cells. In this study, we aimed to determine whether or not another HCV protein(s) transactivates the IL-8 gene expression, by means of an IL-8 promoter-driven luciferase reporter assay and measurement of endogenous IL-8 mRNA and secreted IL-8 protein levels. We observed that NS4B, and NS4A to a lesser extent, significantly transactivated the IL-8 promoter, which resulted in enhanced production of IL-8 protein. Also, the IL-8 expression was augmented in Huh-7 cells harboring an HCV subgenomic RNA replicon, compared with the control cells. Deletion mutational analysis of the IL-8 promoter revealed the possible involvement of the transcription factor AP-1 in both NS4A- and NS4B-mediated IL-8 gene activation. In addition, the IL-8 gene activation by NS4B, but not that by NS4A, was likely to involve NF-κB and/or NFIL-6. The degree of the transactivation by NS4B and NS4A varied with different human cell lines, with HeLa cells showing the strongest activation followed by Huh-7 cells, and with HepG2 cells exhibiting a marginal level of activation. Taken together, our present results suggest the possibility that NS4B and NS4A play an important role in inducing the IL-8 gene expression under certain cellular conditions, which might be one of the strategies to establish persistent HCV infection.**

***Key words*: Hepatitis C virus, Nonstructural proteins, Transactivation, Interleukin 8**

More than 170 million people are infected with hepatitis C virus (HCV), with average prevalence being 2–3% (23). HCV infection is a major cause of chronic hepatitis, liver cirrhosis and hepatocellular carcinoma. Patients infected with HCV are treated with interferon (IFN)-α, alone or in combination with ribavirin (28, 40, 41). HCV is classified into six genotypes. Responsiveness to IFN-ribavirin combination therapy varies with different genotypes. For example, more than 80% of genotypes 2 and 3, but less than 50% of genotypes 1, 4, 5 and 6, were reported to respond well to the treatment (42). The HCV genome is positive-stranded RNA of about 9,600 nucleotides with a large open reading frame (ORF). This ORF encodes a polyprotein precursor of approximately 3,000 amino acid residues, which consists of core protein, envelope proteins (E1 and E2), p7, nonstructural protein 2 (NS2), NS3, NS4A, NS4B, NS5A and NS5B (44).

NS4A, which consists of 54 amino acids, is a cofactor for the NS3 serine protease, forming a stable complex with it at its N-terminal domain (1, 6, 45). NS4A is localized mostly in the endoplasmic reticulum (ER) (21). When coexpressed with NS4A, NS3 is localized

**Address correspondence to* Dr. Hak Hotta, Department of Microbiology, Kobe University Graduate School of Medicine, 7–5–1 Kusunoki-cho, Chuo-ku, Kobe, Hyogo 650–0017, Japan. Fax: +81–78–382–5519. E-mail: hotta@kobe-u.ac.jp

Abbreviations: ATF6β, activating transcription factor 6β; ELISA, enzyme linked immunosorbent assay; ER, endoplasmic reticulum; GRE, glucocorticoid-response element; HCV, hepatitis C virus; HNF-1, hepatocyte nuclear factor 1; IFN, interferon; IL-8, interleukin 8; IRF-1, interferon regulatory factor 1; NFIL-6, nuclear factor IL-6; NF-κB, nuclear factor κB; NS, nonstructural protein; ORF, open reading frame; PCR, polymerase chain reaction; PERK, PKR-like endoplasmic reticulum kinase; RT, reverse transcription; SDS, sodium dodecyl sulfate; TNF-α, tumor necrosis factor α; TRAF2, TNF receptor-associated factor-2.

in membranes of the ER or an ER-like modified compartment (56). NS4B is also a membrane-bound protein of 261 residues, mostly localized in ER (13). We and other researchers have independently reported that NS4A and NS4B inhibit protein synthesis probably through causing ER stress (8, 18). We have also reported that NS4B associates with activating transcription factor 6β (ATF6β), which is known as an ER stress-induced transcription factor (52).

Interleukin 8 (IL-8) is a proinflammatory cytokine consisting of 99 amino acids. IL-8 is induced primarily by IL-1 and tumor necrosis factor α (TNF-α) and is produced by mononuclear phagocytes, fibroblasts, endothelial cells, and a variety of epithelial cells. Many viruses, including cytomegalovirus, Epstein-Barr virus, respiratory syncytial virus, Sendai virus, human immunodeficiency virus and HCV, are reported to induce IL-8 *in vitro* and/or *in vivo* (5, 7, 12, 22, 27, 31, 38, 43). It was also reported that expression of HCV NS5A induced IL-8 expression, leading to partial inhibition of the IFN-induced antiviral response (39). In the present paper, we report that NS4A and NS4B transactivated IL-8 promoter more strongly than NS5A. We also observed that levels of IL-8 mRNA and IL-8 protein were higher in Huh-7 cells harboring HCV RNA replicon than in the control cells.

Materials and Methods

Plasmid construction. An expression plasmid for NS4A (pSG5-NS4A) was constructed as described below. Briefly, a cDNA fragment encoding the full-length NS4A was amplified from the plasmid pFK5B2884Gly by polymerase chain reaction (PCR) using sense (5′-GGAGGAATTCGTCATGAGCAC-CTGGGTGCT-3′) and anti-sense primers (5′-GAG-GAATTCCTAACACTCTTCCATCTCATC-3′). The amplified fragment was digested with *Eco*RI, and subcloned into a unique *Eco*RI site of the pSG5 vector (Stratagene, La Jolla, Calif., U.S.A.). The sequence of the cloned fragment was verified by sequence analysis. pSG5-Core, pSG5-NS3, pSG5-NS4B, pSG5-NS5A and pSG5-NS5B were described previously (8, 15, 49, 54). The plasmid pFK5B2884Gly containing an HCV subgenomic RNA replicon with a cell culture-adaptive Arg-to-Gly mutation at residue 2884 (26) was a kind gift from Dr. R. Bartenschlager, University of Heidelberg, Heidelberg, Germany.

Luciferase reporter plasmids containing serially deleted forms of the IL-8 promoter, such as pIL-8(-1481)Luc, pIL-8(-391)Luc, pIL-8(-335)Luc, pIL-8(-130)Luc, pIL-8(-112)Luc and pIL-8(-6)Luc, were described previously (20, 32) and kindly provided by Dr. H. Nakamura (Seirei Hamamatsu General Hospital, Hamamatsu, Shizuoka, Japan).

Cell culture and plasmid transfection. Human hepatoma-derived Huh-7 and HepG2 cells as well as human uterus cancer-derived HeLa cells were cultured in Dulbecco's modified Eagle's medium supplemented with 10% fetal calf serum. The cells were transfected with plasmids using FuGENE 6 transfection reagent (Roche, Basel, Switzerland), according to the manufacturer's instruction. The cells were then incubated for 24 hr before the analysis.

Huh-7 cell clones stably harboring HCV subgenomic RNA replicon were generated as described previously (26, 51) and maintained in culture medium containing G418 (400 μg/ml).

Reverse transcription (RT) and PCR. RNA was extracted from cultured cells using TRIZOL reagent (Invitrogen, Carlsbad, Calif., U.S.A.), according to the manufacturer's protocol. The RNA obtained was reverse transcribed at 42 C for 60 min using avian myeloblastosis virus reverse transcriptase and random primer (TaKaRa Bio, Shiga, Japan). The resultant cDNAs were heated at 94 C for 5 min, and then amplified with *Pfu* DNA polymerase (Promega, Madison, Wisc., U.S.A.) by PCR cycles (30 to 35 cycles), each consisting of denaturation at 94 C for 45 sec, primer annealing at 55 C for 45 sec and chain elongation at 72 C for 1.5 min. A set of primers, IL-8-S (sense; 5′-ATGACTTCCAAGCTGGCCGTGGCT-3′) and IL-8-AS (antisense; 5′-TCTCAGCCCTCTTCAAAAACT-TCTC-3′), were used to amplify a portion of IL-8 mRNA. Another set of primers, β-actin5 (sense; 5′-CCAACCGCGAGAAGATGAC-3′) and β-actin3 (antisense; 5′-AGAAGCATTTGCGGTGGAC-3′) were used for amplification of β-actin mRNA as a control. The PCR products were electrophoresed in a 1.5% agarose gel containing ethidium bromide and visualized by UV illumination. The expected sizes of the PCR products for IL-8 and β-actin were 289 and 785 base-pairs, respectively.

Luciferase reporter assay. Cells were seeded on a 24-well tissue culture plate. After 12 hr, the cells were co-transfected with 100 ng of each of the HCV plasmids or an empty control vector, 100 ng of a reporter plasmid that expresses firefly luciferase under the control of the IL-8 promoter (see above) and 1 ng of pRL-SV40 (Promega) that expresses *Renilla* luciferase as an internal control, using FuGENE 6. Duplicate or triplicate cultures were prepared for each experiment. In experiments where cells harboring HCV subgenomic RNA replicon were used, the HCV plasmids were omitted from the transfection. After 24 hr, cell lysates were prepared using Passive Lysis Buffer (Promega) and 10

μl of the lysate was used for dual luciferase assay, according to the manufacturer's instruction. Luciferase activities were measured by using Luminescencer JNR AB-2100 (Atto, Tokyo). Firefly luciferase activities in each cell lysate were normalized to *Renilla* luciferase activities.

Measurement of secreted IL-8 protein levels and total cellular protein levels. IL-8 protein levels in cell culture supernatants were determined using commercially available enzyme linked immunosorbent assay (ELISA) kit (R&D Systems, Minneapolis, Minn., U.S.A.). As a control, cells were lysed in Passive Lysis Buffer (Promega) and amounts of total cellular proteins in the lysates were determined using commercially available BCA Protein Assay Reagent Kit (Pierce, Rockford, Ill., U.S.A.). Secreted IL-8 protein levels in each culture were normalized to total protein levels in the cell lysates.

Results

HCV NS4A and NS4B Transactivate the IL-8 Promoter

By means of luciferase reporter assay using pIL-8 (-391)Luc, we first determined whether or not HCV proteins transactivate IL-8 promoter. The results obtained demonstrated that NS4B and NS4A each markedly transactivated IL-8 promoter, with the former more prominently than the latter (Fig. 1). The other HCV proteins, such as Core, NS3, NS5A and NS5B, exerted marginal effects, if any, under this experimental condition. Similar results were obtained using pIL-8 (-1481)Luc (data not shown).

Next, we determined possible transactivating effects of NS4B and NS4A, in parallel with NS5A, on the authentic IL-8 promoter by measuring endogenous IL-8 mRNA levels. The result showed that endogenous IL-8 mRNA levels were significantly elevated in cells expressing NS4B and those expressing NS4A, compared to the control (Fig. 2, A and B). Consistently, amounts of secreted IL-8 protein in culture supernatants of cells expressing NS4A and NS4B were larger than that in the control (Fig. 2C). Also, NS5A-expressing cells produced more amount of IL-8 protein than did the control.

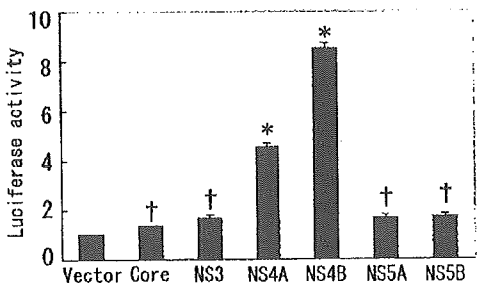

Fig. 1. Transactivating effects of HCV proteins on IL-8 promoter in the luciferase reporter gene. Each HCV expression plasmid or an empty vector as a control was cotransfected with pIL-8 (-391)Luc and pRL-SV40 plasmid into Huh-7 cells. After 24 hr, the cells were lysed and luciferase activities in the cell lysates were determined, as described in "Materials and Methods." The vertical axis indicates arbitrary units of luciferase activities. Data represent the mean±SD obtained from three separate experiments. *, $P<0.001$, compared to the control; †, $P<0.05$, compared to the control.

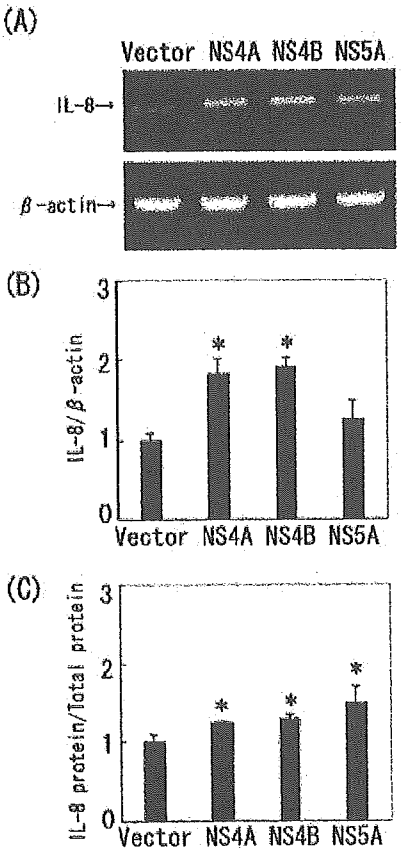

Fig. 2. Transactivating effects of NS4A, NS4B and NS5A on the authentic promoter of the IL-8 gene. (A) Amounts of IL-8 mRNA in Huh-7 cells transfected with each HCV expression plasmid or an empty vector were analyzed by RT-PCR. A representative result of three separate experiments is shown. (B) IL-8 mRNA levels shown in (A) were quantitated using the NIH image 1.61 software and normalized to β-actin mRNA levels. Data represent the mean±SD obtained from three separate experiments. *, $P<0.05$, compared to the control. (C) Secreted IL-8 protein levels in the culture supernatants of the cells in (A) were measured using an ELISA kit. Secreted IL-8 protein levels in each culture were normalized to total protein levels in the cell lysates. Data represent the mean±SD obtained from three separate experiments. *, $P<0.05$, compared to the control.

HCV Subgenomic RNA Replicon Transactivates the IL-8 Promoter and Augments IL-8 Production in Huh-7 Cells

In HCV-infected cells, NS4A and NS4B form a complex with NS3, NS5A and NS5B, which functions as the RNA replication machinery (15, 24). As replication of HCV RNA replicon mimics HCV infection, we measured IL-8 promoter activity in Huh-7 cells harboring HCV subgenomic RNA replicon, and compared it with that in the control cells. The result demonstrated that the IL-8 promoter activity, as measured by using pIL-8(-391)Luc, was significantly stronger in HCV RNA replicon-harboring cells than in the control cells (Fig. 3). Similar results were obtained using pIL-8 (-1481)Luc (data not shown).

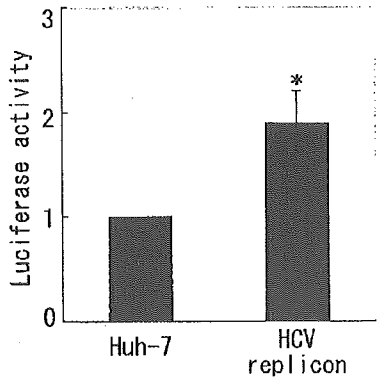

Fig. 3. Transactivating effects of HCV subgenomic RNA replicon on IL-8 promoter in the luciferase reporter gene. pIL-8 (-391)Luc and pRL-SV40 plasmid were cotransfected into Huh-7 cells harboring HCV subgenomic RNA replicon and the control cells. After 24 hr, the cells were lysed and luciferase activities in the cell lysates were determined. Data represent the mean±SD obtained from two separate experiments. *, $P<0.05$, compared to the control.

We then measured endogenous IL-8 mRNA levels by RT-PCR. The result obtained revealed that IL-8 mRNA levels were higher in cells harboring HCV subgenomic RNA replicon than in the control cells (Fig. 4, A and B). Consistently, more amounts of IL-8 protein were produced in, and secreted from, HCV RNA replicon-harboring cells compared to the control (Fig. 4B).

Identification of NS4A- and NS4B-Responsive Elements in the IL-8 Promoter Sequence

It has been reported that the IL-8 promoter contains sequences responsible for binding of certain transcription factors, such as interferon regulatory factor 1 (IRF-1), hepatocyte nuclear factor 1 (HNF-1), glucocorticoid-response element (GRE), AP-1, nuclear factor IL-6 (NFIL-6) and nuclear factor κB (NF-κB) (30, 35, 36). The binding sites for those transcription factors are shown in Fig. 5A. We were interested to know which binding site(s) is responsible for the NS4A- and NS4B-mediated transactivation of the IL-8 promoter. The result demonstrated that NS4B-mediated transactivation was significantly more prominent with pIL-8(-130)Luc than with pIL-8(-335)Luc and pIL-8(-112)Luc (Fig. 5B). Also, there was a significant reduction in NS4B-

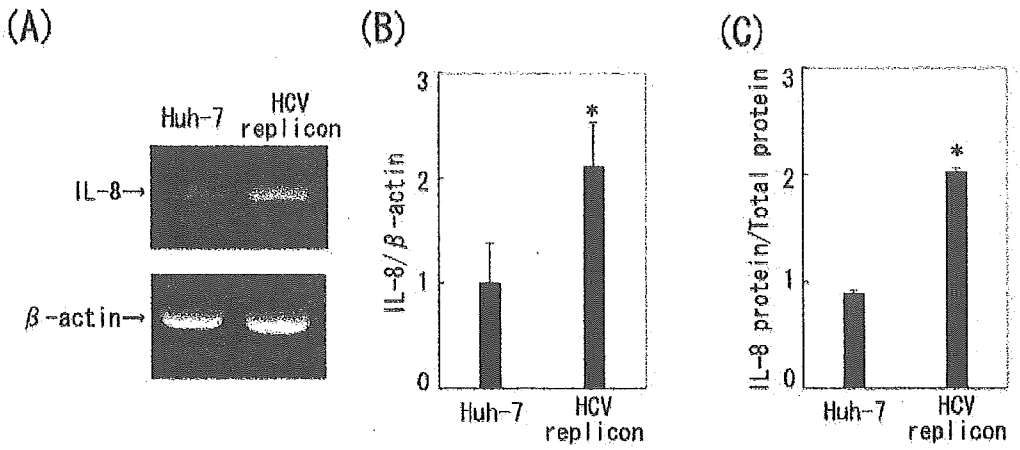

Fig. 4. Transactivating effects of HCV subgenomic RNA replicon on the authentic promoter of the IL-8 gene. (A) IL-8 mRNA levels in Huh-7 cells harboring HCV subgenomic RNA replicon and the control cells were analyzed by RT-PCR. A representative result of three separate experiments is shown. (B) IL-8 mRNA levels shown in (A) were quantitated using the NIH image 1.61 software and normalized to β-actin mRNA levels. Data represent the mean±SD obtained from three separate experiments. *, $P<0.05$, compared to the control. (C) Secreted IL-8 protein levels in culture supernatants of Huh-7 cells harboring HCV subgenomic RNA replicon and the control cells were measured using an ELISA kit. Secreted IL-8 protein levels in each culture were normalized to total protein levels in the cell lysates. Data represent the mean±SD obtained from three separate experiments. *, $P<0.05$, compared to the control.

mediated transactivation when pIL-8(-112)Luc was further truncated. These results suggest the possible presence of an NS4B-responsive suppressor sequence(s) between −335 and −130 of the IL-8 promoter and at least two distinct NS4B-responsive enhancer sequences, one between −130 and −112, and the other between −112 and −6. It is likely that the AP-1 binding site (−126 to −120) and either one of the NFIL-6 binding site (−94 to −81) or the NF-κB binding site (−81 to −71), or both, are involved in the NS4B-mediated transactivation. In this connection, it was reported that NS4B transactivated the NF-κB- and AP-1-mediated promoter activities (17).

As for the NS4A-mediated transactivation, a significant difference was observed when pIL-8(-130)Luc and pIL-8(-112)Luc NS4A were compared. This result suggests the possible involvement of the AP-1 binding site (−126 to −120) in the NS4A-mediated transactivation. Alternatively, there may be another enhancer sequence involved in this transactivation since it was reported that NS4A barely, if any, transactivated AP-1- and NF-κB-mediated promoter activity (17).

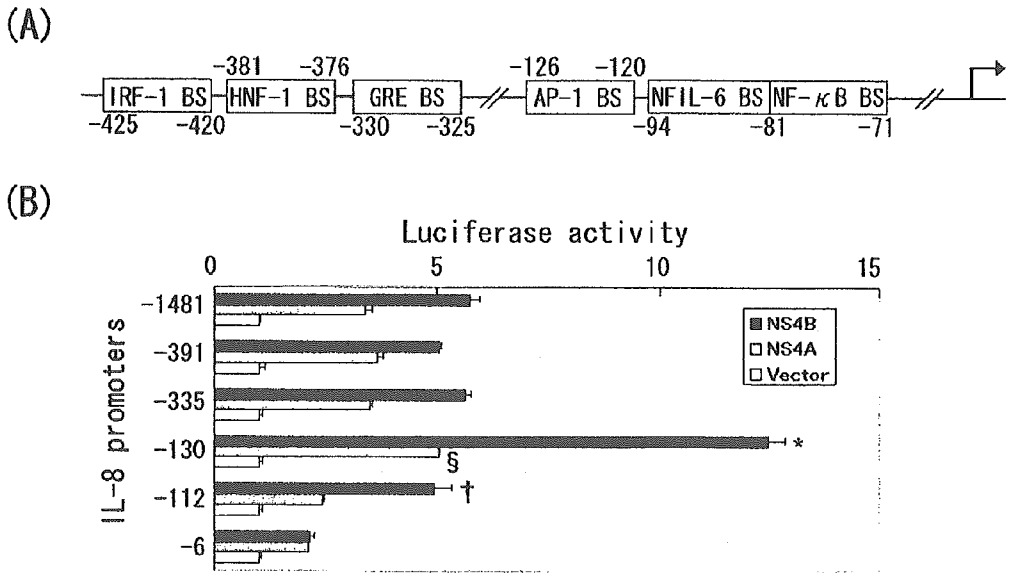

Fig. 5. Transactivating effects of NS4A and NS4B on serially truncated forms of IL-8 promoters in the luciferase reporter gene. (A) Potential binding sites (BS) for known transcriptional factors are depicted. (B) Each HCV expression plasmid or an empty vector was cotransfected into Huh-7 cells together with a reporter plasmid each containing serially truncated forms of IL-8 promoter (see "Materials and Methods") and pRL-SV40. After 24 hr, the cells were lysed and luciferase activities in the cell lysates were determined. The vertical axis indicates fold activation of the luciferase activities by NS4A and NS4B over the control (vector). Data represent the mean±SD obtained from two separate experiments. *, $P<0.001$, compared to pIL-8(-335)Luc and pIL-8(-112)Luc; †, $P<0.001$, compared to pIL-8(-6) Luc; §, $P<0.001$, compared to pIL-8(-112) Luc.

Table 1. Differential transactivating effects of HCV proteins on IL-8 promoter in different human cell lines

Cell	Fold activation (luciferase activity)			
	Vector	NS4A	NS4B	NS5A
Huh-7	1.00±0.05	3.0±0.5*	4.6±0.6*	1.2±0.1†
HepG2	1.00±0.09	1.6±0.1*	1.7±0.3†	1.1±0.2
HeLa	1.00±0.05	14.6±1.1*	24.1±0.2*	1.4±0.1*

Each HCV plasmid or an empty vector (control) was cotransfected with pIL-8(-391)Luc and pRL-SV40 into Huh-7, HepG2 and HeLa cells. After 24 hr, the cells were lysed and luciferase activities in the cell lysates were determined, as described in "Materials and Methods." Fold activation of the luciferase activities by HCV proteins over control (vector) was calculated. Data represent the mean±SD obtained from two separate experiments. *, $P<0.001$, compared to the control; †, $P<0.05$, compared to the control.

The Degree of NS4A- and NS4B-Transactivation of the IL-8 Promoter Varies with Different Human Cell Lines

As transcriptional activation depends largely on cell types tested, we compared three different human cell lines, Huh-7, HepG2 and HeLa, in terms of HCV protein-mediated transactivation of the IL-8 promoter using pIL-8(-391)Luc. Although a moderate degree (3- to 5-fold) of transcriptional activation by NS4B and NS4A was repeatedly observed in Huh-7 cells, only a marginal degree (<1.7-fold) of transcriptional activation was observed in HepG2 cells transfected with NS4B and NS4A (Table 1). On the other hand, transcriptional activation by NS4B and NS4A was much more prominent in HeLa cells (15- to 24-fold) than in Huh-7 cells. It should also be noted that NS4B and NS4A exerted stronger effects than NS5A in all three cell lines tested.

Despite the prominent activation on pIL-8(-391)Luc in HeLa cells, expression levels of endogenous IL-8 mRNA were much lower than in Huh-7 cells and, consequently, production of IL-8 protein in culture supernatants of HeLa cells was below a minimal detectable level, irrespective of HCV protein expression, under the same experimental condition for Huh-7 cells (data not shown). In this connection, it was previously reported that Huh-7 cells produced high levels of IL-8 (29).

Discussion

Possible pathogenetic association of IL-8 with HCV infection has been documented to date. Polyak et al. (38) reported that serum IL-8 levels were significantly higher in HCV-infected patients than in uninfected individuals. It was also reported that HCV NS5A augmented IL-8 expression (39, 46). Moreover, intrahepatic IL-8 mRNA levels were positively correlated with severity of hepatic inflammation and injury in patients with chronic hepatitis C (9, 48).

In the present study, we investigated possible transactivating effects of HCV proteins (Core, NS3, NS4A, NS4B, NS5A, NS5B) on the IL-8 promoter and found that NS4B, and NS4A to a lesser extent, significantly transactivated the IL-8 promoter, as determined by luciferase reporter assay and IL-8 mRNA levels (Figs. 1 and 2A). Consistently, we observed a slight, but statistically significant increase in the amount of secreted IL-8 protein in NS4B- and NS4A-transfected cell cultures (Fig. 2C). It should also be noted that, despite its weaker effect on the IL-8 promoter, NS5A exerted a comparable degree of increase in secreted IL-8 protein levels. A plausible explanation for this is that NS4B and NS4A as well as core protein of HCV, but not NS5A, suppress protein synthesis at the translation level (8, 18, 34) and that the amount of secreted IL-8 protein is determined by the balance between transcriptional activation and translational suppression by NS4B and NS4A.

Since its establishment in 1999 (25), HCV subgenomic RNA replicon system has been widely used to investigate the viral replication mechanism and functional features of the viral proteins (2, 10, 33, 50, 55). Using such a system, we demonstrated that IL-8 promoter was transactivated by HCV subgenomic RNA replicon (Figs. 3 and 4 A) and that secreted IL-8 protein levels were significantly greater in the HCV subgenomic RNA replicon-harboring cells than in the control (Fig. 4C). It is conceivable that both transcriptional activation and translational suppression by NS4B (or NS4A) are weaker in cells stably harboring HCV RNA replicon than in cells transiently expressing NS4B (or NS4A) alone, due to the fact that NS4B and NS4A are incorporated into the replication complex together with the other HCV proteins and do not freely associate with host cell proteins. As stated above, the balance between transcriptional activation and translational suppression would determine the degree of IL-8 protein production and we assume that transcriptional activation by NS4B surpasses translational suppression by the same protein in HCV RNA replicon-harboring cells. The present results obtained with HCV subgenomic RNA replicon are in line with a recent observation that HCV infection induced IL-8 production in cultured human macrophages (43). On the other hand, it should be noted that, despite our effort to avoid it, we cannot completely exclude the possibility of clonal difference between the HCV RNA replicon-harboring cells and the control. Also, we should consider the possible involvement of HCV structural proteins in the pathogenesis of HCV infection. HCV full-length genomic RNA replicon systems are now available (4, 14, 37) and experiments using such a system would provide us with more information on HCV infection-mediated IL-8 induction.

NS4B and NS4A each suppress translation probably through ER stress (8). Upon ER stress, IRE1, PKR-like ER kinase (PERK) and ATF6 are activated (3, 47). Mammalian cells have two IRE1 isoforms, referred to as IRE1α and IRE1β. The cytoplasmic part of IRE1s interacts with TNF receptor-associated factor-2 (TRAF2), an adaptor protein that couples plasma membrane receptors to JNK activation (53). In addition, TRAF2 is involved in TNF-α signaling cascade, leading to NF-κB activation and IL-8 expression (16). Thus, ER stress, which is caused under a variety of circumstances, including virus infection, induces upregulation of IL-8 expression. This mechanism is likely to be involved in the NS4A- and NS4B-mediated transactivation of the IL-8 promoter.

Specific binding sites for a number of transcription factors, such as AP-1, NF-κB and NFIL-6, have been identified within the IL-8 promoter sequence (see Fig. 5A) and these factors would transactivate the IL-8 promoter. It is well known that NF-κB is activated by a large number of extracellular stimuli, including LPS, TNF-α, IL-1 and viral infection, through phosphorylation and proteasome-dependent degradation of IκB (11), and that NF-κB regulates inflammatory responses and expression of not only IL-8 but also various other cytokines, such as IL-1, -2, -3, -6, -12, TNF-α and IFN-β. Our present results suggest that NS4B induces IL-8 gene expression through AP-1, NF-κB and/or NFIL-6 (Fig. 5), which is consistent with a previous report showing that NS4B activated NF-κB-associated signal (17). Activation of NF-κB-associated signal in cells harboring HCV subgenomic RNA replicon was also reported by other investigators (55). The same authors claimed that NS5A was responsible for the NF-κB activation. However, possible effects of either NS4A or NS4B were not tested in their experiments.

IL-8 is known to inhibit antiviral activity of IFN-α (19). Namba et al. (33) recently reported that IFN-resistant HCV RNA replicons possessed a common amino acid substitution in NS4B and a number of amino acid substitutions in NS5A, suggesting that those mutations are involved in the IFN resistance. Our present results and observations of other researchers (39) imply the possibility that HCV infection, through the function of NS4B, NS4A and possibly NS5A, upregulates the IL-8 gene expression. Our results also demonstrated that the degree of the IL-8 gene activation by NS4B and NS4A varied with different human cell lines, with HeLa cells showing the strongest activation followed by Huh-7 cells, and with HepG2 cells exhibiting a marginal level of activation. Taken together, the present results suggest the possibility that NS4B and NS4A play an important role in inducing the IL-8 gene expression under certain cellular conditions, which might be one of the viral strategies to counteract antiviral activity of IFN, eventually leading to the establishment of persistent HCV infection.

We are grateful to Dr. R. Bartenschlager (University of Heidelberg, Heidelberg, Germany) for providing pFK5B2884Gly. Thanks also due to Dr. H. Nakamura (Seirei Hamamatsu General Hospital, Hamamatsu, Shizuoka, Japan) for providing pIL-8(-1481)Luc, pIL-8(-391)Luc, pIL-8(-335)Luc, pIL-8(-130)Luc, pIL-8(-112)Luc and pIL-8(-6)Luc. This work was supported in part by Grants-in-Aid for Scientific Research from the Ministry of Education, Culture, Sports, Science and Technology, Japan, and the Japan Society for the Promotion of Science.

References

1) Bartenschlager, R., Lohmann, V., Wilkinson, T., and Koch, J.O. 1995. Complex formation between the NS3 serine-type proteinase of the hepatitis C virus and NS4A and its importance for polyprotein maturation. J. Virol. **69**: 7519–7528.
2) Bartenschlager, R., Kaul, A., and Sparacio, S. 2003. Replication of the hepatitis C virus in cell culture. Antiviral Res. **60**: 91–102.
3) Bertolotti, A., Zhang, Y., Hendershot, L.M., Harding, H.P., and Ron, D. 2000. Dynamic interaction of BiP and ER stress transducers in the unfolded-protein response. Nat. Cell Biol. **2**: 326–332.
4) Blight, K.J., McKeating, J.A., and Rice, C.M. 2002. Highly permissive cell lines for subgenomic and genomic hepatitis C virus RNA replication. J. Virol. **76**: 13001–13014.
5) Booth, L.J., and Metcalf, J.P. 1999. Type-specific induction of interleukin-8 by adenovirus. Am. J. Respir. Cell Mol. Biol. **21**: 521–527.
6) Failla, C., Tomei, L., and De Francesco, R. 1995. An amino-terminal domain of the hepatitis C virus NS3 protease is essential for interaction with NS4A. J. Virol. **69**: 1769–1777.
7) Fiedler, M.A., Wernke-Dollries, K., and Stark, J.M. 1995. Respiratory syncytial virus increases IL-8 gene expression and protein release in A549 cell. Am. J. Physiol. **269**: 865–872.
8) Florese, H.R., Nagano-Fujii, M., Iwanaga, Y., Hidajat, R., and Hotta, H. 2002. Inhibition of protein synthesis by the nonstructural proteins NS4A and NS4B of hepatitis C virus. Virus Res. **90**: 119–131.
9) Fukuda, R., Ishimura, N., Ishihara, S., Chowdhury, A., Moriyama, N., Nogami, C., Miyake, T., Niigaki, M., Tokuda, A., Satoh, S., Sakai, S., Akagi, S., Watanabe, M., and Fukumoto, S. 1996. Intrahepatic expression of pro-inflammatory cytokine mRNAs and interferon efficacy in chronic hepatitis C. Liver **16**: 390–399.
10) Gao, L., Aizaki, H., He, J.W., and Lai, M.M. 2004. Interactions between viral nonstructural proteins and host protein hVAP-33 mediate the formation of hepatitis C virus RNA replication complex on lipid raft. J. Virol. **78**: 3480–3488.
11) Ghosh, S., and Baltimore, D. 1990. Activation *in vitro* of NF-κB by phosphorylation of its inhibitor IκB. Nature **344**: 678–682.
12) Hua, J., Liao, M.J., and Rashidbaigi, A. 1996. Cytokines induced by Sendai virus in human peripheral blood leukocytes. J. Leukoc. Biol. **60**: 125–128.
13) Hügle, T., Fehrmann, F., Bieck, E., Kohara, M., Kräusslich, H.G., Rice, C.M., Blum, H.E., and Moradpour, D. 2001. The hepatitis C virus nonstructural protein 4B is an integral endoplasmic reticulum membrane protein. Virology **25**: 70–81.
14) Ikeda, M., Yi, M., Li, K., and Lemon, S.M. 2002. Selectable subgenomic and genome-length dicistronic RNAs derived from an infectious molecular clone of the HCV-N strain of hepatitis C virus replicate efficiently in cultured Huh7 cells. J. Virol. **76**: 2997–3006.
15) Ishido, S., Fujita, T., and Hotta, H. 1998. Complex forma-

tion of NS5B with NS3 and NS4A proteins of hepatitis C virus. Biochem. Biophys. Res. Commun. **6**: 35–40.

16) Jobin, C., Holt, L., Bradham, C.A., Streetz, K., Brenner, D.A., and Sartor, R.B. 1999. TNF receptor-associated factor-2 is involved in both IL-1 beta and TNF-alpha signaling cascades leading to NF-κB activation and IL-8 expression in human intestinal epithelial cells. J. Immunol. **162**: 4447–4454.
17) Kato, N., Yoshida, H., Kioko, Ono-Nita, S., Kato, J., Goto, T., Otsuka, M., Lan, K., Matsushima, K., Shiratori, Y., and Omata, M. 2000. Activation of intracellular signaling by hepatitis B and C viruses: C-viral core is the most potent signal inducer. Hepatology **32**: 405–412.
18) Kato, J., Kato, N., Yoshida, H., Ono-Nita, K.S., Shiratori, Y., and Omata, M. 2002. Hepatitis C virus NS4A and NS4B proteins suppress translation *in vivo*. J. Med. Virol. **66**: 187–199.
19) Khabar, K.S., Al-Zoghaibi, F., Murayama, T., Matsushima, K., Mukaida, N., Siddiqui, Y., Dhalla, M., and Al-Ahdal, M.N. 1997. Interleukin-8 selectively enhances cytopathic effect (CPE) induced by positive-strand RNA viruses in the human WISH cell line. Biochem. Biophys. Res. Commun. **235**: 774–778.
20) Kikuchi, T., Hagiwara, K., Honda, Y., Gomi, K., Kobayashi, T., Takahashi, H., Tokue, Y., Watanabe, A., and Nukiwa, T. 2002. Clarithromycin suppresses lipopolysaccharide-induced interleukin-8 production by human monocytes through AP-1 and NF-kappa B transcription factors. J. Antimicrob. Chemother. **49**: 745–755.
21) Kim, J.E., Song, W.K., Chung, K.M., Back, S.H., and Jang, S.K. 1991. Subcellular localization of hepatitis C viral proteins in mammalian cells. Arch. Virol. **144**: 329–343.
22) Kutsch, O., Oh, J., Nath, A., and Benveniste, E.N. 2000. Induction of the chemokines interleukin-8 and IP-10 by human immunodeficiency virus type 1 Tat in astrocytes. J. Virol. **74**: 9214–9221.
23) Lauer, G.M., and Walker, B.D. 2001. Hepatitis C virus infection. N. Engl. J. Med. **345**: 41–52.
24) Lin, C., Wu, J.W., Hsiao, K., and Su, M.S. 1997. The hepatitis C virus NS4A protein: interactions with the NS4B and NS5A proteins. J. Virol. **71**: 6465–6471.
25) Lohmann, V., Korner, F., Koch, J., Herian, U., Theilmann, L., and Bartenschlager, R. 1999. Replication of subgenomic hepatitis C virus RNAs in a hepatoma cell line. Science **285**: 110–113.
26) Lohmann, V., Korner, F., Dobierzewska, A., and Bartenschlager, R. 2001. Mutations in hepatitis C virus RNAs conferring cell culture adaptation. J. Virol. **75**: 1437–1449.
27) McColl, S.R., Roberge, C.J., Larochelle, B., and Gosselin, J. 1997. EBV induces the production and release of IL-8 and macrophage inflammatory protein-1 α in human neutrophils. J. Immunol. **159**: 64–68.
28) McHutchison, J.G., Gordon, S.C., Schiff, E.R., Shiffman, M.L., Lee, W.M., Rustgi, V.K., Goodman, Z.D., Ling, M.H., Cort, S., and Albrecht, J.K. 1998. Interferon alfa-2b alone or in combination with ribavirin as initial treatment for chronic hepatitis C. N. Engl. J. Med. **339**: 1485–1492.
29) Miyamoto, M., Shimizu, Y., Okada, K., Kashii, Y., Higuchi, K., and Watanabe, A. 1998. Effect of interleukin-8 on production of tumor-associated substances and autocrine growth of human liver and pancreatic cancer cells. Cancer Immunol. Immunother. **47**: 47–57.
30) Mukaida, N., Mahe, Y., and Matsushima, K. 1990. Cooperative interaction of nuclear factor-kappa B- and cis-regulatory enhancer binding protein-like factor binding elements in activating the interleukin-8 gene by pro-inflammatory cytokines. J. Biol. Chem. **265**: 21128–21133.
31) Murayama, T., Ohara, Y., Obuchi, M., Khabar, K.S., Higashi, H., Mukaida, N., and Matsushima, K. 1997. Human cytomegalovirus induces interleukin-8 production by a human monocytic cell line, THP-1, through acting concurrently on AP-1- and NF-κB-binding sites of the interleukin-8 gene. J. Virol. **71**: 5692–5695.
32) Nakamura, H., Yoshimura, K., Jaffe, H.A., and Crystal, R.G. 1991. Interleukin-8 gene expression in human bronchial epithelial cells. J. Biol. Chem. **266**: 19611–19617.
33) Namba, K., Naka, K., Dansako, H., Nozaki, A., Ikeda, M., Shiratori, Y., Shimotohno, K., and Kato, N. 2004. Establishment of hepatitis C virus replicon cell lines possessing interferon-resistant phenotype. Biochem. Biophys. Res. Commun. **323**: 299–309.
34) Oka, K., Nagano-Fujii, M., Yoshida, I., Hidajat, R., Deng, L., Akutsu, M., and Hotta, H. 2003. Hepatitis C virus core protein selectively inhibits synthesis and accumulation of p21/Waf1 and certain nuclear proteins. Microbiol. Immunol. **47**: 429–438.
35) Okamoto, S., Mukaida, N., Yasumoto, K., Rice, N., Ishikawa, Y., Horiguchi, H., Murakami, S., and Matsushima, K. 1994. The interleukin-8 AP-1 and kappa B-like sites are genetic end targets of FK506-sensitive pathway accompanied by calcium mobilization. J. Biol. Chem. **269**: 8582–8589.
36) Ondrey, F.G., Dong, G., Sunwoo, J., Chen, Z., Wolf, J.S., Crowl-Bancroft, C.V., Mukaida, N., and Van Waes, C. 1999. Constitutive activation of transcription factors NF(kappa)B, AP-1, and NF-IL6 in human head and neck squamous cell carcinoma cell lines that express pro-inflammatory and pro-angiogenic cytokines. Mol. Carcinog. **26**: 119–129.
37) Pietschmann, T., Lohmann, V., Kaul, A., Krieger, N., Rinck, G., Rutter, G., Strand, D., and Bartenschlager, R. 2002. Persistent and transient replication of full-length hepatitis C virus genomes in cell culture. J. Virol. **76**: 4008–4021.
38) Polyak, S.J., Khabar, K.S., Rezeiq, M., and Gretch, D.R. 2001. Elevated levels of interleukin-8 in serum are associated with hepatitis C virus infection and resistance to interferon therapy. J. Virol. **75**: 6209–6211.
39) Polyak, S.J., Khabar, K.S., Paschal, D.M., Ezelle, H.J., Duverlie, G., Barber, G.N., Levy, D.E., Mukaida, N., and Gretch, D.R. 2001. Hepatitis C virus nonstructural 5A protein induces interleukin-8, leading to partial inhibition of the interferon-induced antiviral response. J. Virol. **75**: 6095–6106.
40) Poynard, T., Marcellin, P., Lee, S., Niederau, C., Minuk, G.S., Ideo, G., Bain, V., Heathcote, J., Zeuzem, S., Trepo, C., and Albrecht, J. 1998. Randomised trial of interferon

α2b plus ribavirin for 48 weeks or for 24 weeks versus interferon α2b plus placebo for 48 weeks for treatment of chronic infection with hepatitis C virus. Lancet **352**: 1426–1432.

41) Poynard, T., McHutchison, J., Goodman, Z., Ling, M.H., and Albrecht, J. 2000. Is an "a la carte" combination interferon alfa-2b plus ribavirin regimen possible for the first line treatment in patients with chronic hepatitis C? Hepatology **31**: 211–218.
42) Poynard, T., Yuen, M.-F., Ratziu, V., and Lai, C.L. 2003. Viral hepatitis C. Lancet **362**: 2095–2100.
43) Radkowski, M., Bednarska, A., Horban, A., Stanczak, J., Wilkinson, J., Adair, D.M., Nowicki, M., Rakela, J., and Laskus, T. 2004. Infection of primary human macrophages with hepatitis C virus *in vitro*: induction of tumour necrosis factor-alpha and interleukin 8. J. Gen. Virol. **85**: 47–59.
44) Reed, K.E., and Rice, C.M. 2000. Overview of hepatitis C virus genome structure, polyprotein processing, and protein properties. Curr. Top. Microbiol. Immunol. **242**: 55–84.
45) Satoh, S., Tanji, Y., Hijikata, M., Kimura, K., and Shimotohno, K. 1995. The N-terminal region of hepatitis C virus nonstructural protein 3 (NS3) is essential for stable complex formation with NS4A. J. Virol. **69**: 4255–4260.
46) Sen, A., Steele, R., Ghosh, A.K., Basu, A., Ray, R., and Ray, R.B. 2003. Inhibition of hepatitis C virus protein expression by RNA interference. Virus Res. **96**: 27–35.
47) Shen, J., Chen, X., Hendershot, L., and Prywes, R. 2002. ER stress regulation of ATF6 localization by dissociation of BiP/GRP78 binding and unmasking of Golgi localization signals. Dev. Cell **3**: 99–111.
48) Shimoda, K., Begum, N.A., Shibuta, K., Mori, M., Bonkovsky, H.L., Banner, B.F., and Barnard, G.F. 1998. Interleukin-8 and hIRH (SDF1-α/PBSF) mRNA expression and histological activity index in patients with chronic hepatitis C. Hepatology **28**: 108–115.
49) Song, J., Fujii, M., Wang, F., Itoh, M., and Hotta, H. 1999. The NS5A protein of hepatitis C virus partially inhibits the antiviral activity of interferon. J. Gen. Virol. **80**: 879–886.
50) Taguchi, T., Nagano-Fujii, M., Akutsu, M., Kadoya, H., Ohgimoto, S., Ishido, S., and Hotta, H. 2004. Hepatitis C virus NS5A protein interacts with 2′, 5′-oligoadenylate synthetase and inhibits antiviral activity of IFN in an IFN sensitivity-determining region-independent manner. J. Gen. Virol. **85**: 959–969.
51) Takigawa, Y., Nagano-Fujii, M., Deng, L., Hidajat, R., Tanaka, M., Mizuta, H., and Hotta, H. 2004. Suppression of hepatitis C virus replicon by RNA interference directed against the NS3 and NS5B regions of the viral genome. Microbiol. Immunol. **48**: 591–598.
52) Tong, W.Y., Nagano-Fujii, M., Hidajat, R., Deng, L., Takigawa, Y., and Hotta, H. 2002. Physical interaction between hepatitis C virus NS4B protein and CREB-RP/ATF6β. Biochem. Biophys. Res. Commun. **6**: 366–372.
53) Urano, F., Wang, X., Bertolotti, A., Zhang, Y., Chung, P., Harding, H.P., and Ron, D. 2000. Coupling of stress in the ER to activation of JNK protein kinases by transmembrane protein kinase IRE1. Science **287**: 664–666.
54) Wang, F., Yoshida, I., Takamatsu, M., Ishido, S., Fujita, T., Oka, K., and Hotta, H. 2000. Complex formation between hepatitis C virus core protein and p21Waf1/Cip1/Sdi1. Biochem. Biophys. Res. Commun. **5**: 479–484.
55) Waris, G., Livolsi, A., Imbert, V., Peyron, J.F., and Siddiqui, A. 2003. Hepatitis C virus NS5A and subgenomic replicon activate NF-kappaB via tyrosine phosphorylation of Ikappa-Balpha and its degradation by calpain protease. J. Biol. Chem. **278**: 40778–40787.
56) Wölk, B., Sansonno, D., Kräusslich, H.G., Dammacco, F., Rice, C.M., Blum, H.E., and Moradpour, D. 2000. Subcellular localization, stability, and *trans*-cleavage competence of the hepatitis C virus NS3-NS4A complex expressed in tetracycline-regulated cell lines. J. Virol. **74**: 2293–2304.

Wild-Type Measles Virus Infection in Human CD46/CD150-Transgenic Mice: CD11c-Positive Dendritic Cells Establish Systemic Viral Infection[1]

Masashi Shingai,[2*†] Naokazu Inoue,[2‡] Tsuyoshi Okuno,[‡] Masaru Okabe,[‡] Takashi Akazawa,[*] Yasuhide Miyamoto,[*] Minoru Ayata,[§] Kenya Honda,[¶] Mitsue Kurita-Taniguchi,[*] Misako Matsumoto,[*†] Hisashi Ogura,[§] Tadatsugu Taniguchi,[¶] and Tsukasa Seya[3†]

We generated transgenic (TG) mice that constitutively express human CD46 (huCD46) and/or TLR-inducible CD150 (huCD150), which serve as receptors for measles virus (MV). These mice were used to study the spreading and pathogenicity of GFP-expressing or intact laboratory-adapted Edmonston and wild-type Ichinose (IC) strains of MV. Irrespective of the route of administration, neither type of MV was pathogenic to these TG mice. However, in ex vivo, limited replication of IC was observed in the spleen lymphocytes from huCD46/huCD150 TG and huCD150 TG, but not in huCD46 TG and non-TG mice. In huCD150-positive TG mouse cells, CD11c-positive bone marrow-derived myeloid dendritic cells (mDC) participated in MV-mediated type I IFN induction. The level and induction profile of IFN-β was higher in mDC than the profile of IFN-α. Wild-type IC induced markedly high levels of IFN-β compared with Edmonston in mDC, as opposed to human dendritic cells. We then generated huCD46/huCD150 TG mice with type I IFN receptor (IFNAR1)$^{-/-}$ mice. MV-bearing mDCs spreading to draining lymph nodes were clearly observed in these triple mutant mice in vivo by i.p. MV injection. Infectious lymph nodes were also detected in the double TG mice into which MV-infected CD11c-positive mDCs were i.v. transferred. This finding suggests that in the double TG mouse model mDCs once infected facilitate systemic MV spreading and infection, which depend on mDC MV permissiveness determined by the level of type I IFN generated via IFNAR1. Although these results may not simply reflect human MV infection, the huCD150/huCD46 TG mice may serve as a useful model for the analysis of MV-dependent modulation of mDC response. *The Journal of Immunology,* **2005, 175: 3252–3261.**

Measles virus (MV)[4] causes severe immune suppression followed by secondary infections that result in high rates of mortality of infants particularly in developing countries. Human CD46 (huCD46) (1, 2) and TLR-inducible human CD150 (huCD150) (3, 4) have been identified as MV receptors. Although huCD150 is the primary entry receptor for MV, it is not expressed in epithelial cells of the respiratory tract through which MV infection is known to initiate. The mechanism of wild-type MV spreading to systemic organs, therefore, remains unsolved.

No entry receptor for MV has been identified in mice. MV tropism is represented by its receptors, huCD46 and huCD150. Although rodents express the orthologues of these receptors, they fail to act as entry receptors for MV (2, 5, 6). MV infection of adult rodents is restricted to the brain-adapted strains obtained by intracerebral inoculations (7, 8). Transgenic (TG) mice expressing either huCD46 (9–11) or huCD150 (12, 13) have been established as models to investigate MV pathogenicity. Initially, most of the studies were performed using huCD46 TG mice. MV entry was found to be more efficient in mouse cells that express huCD46, the receptor for the MV vaccine Edmonston (ED) strain (1), and probably for several wild-type strains as well (14). However, TG rodents expressing huCD46 are not susceptible to MV infection when inoculated by routes other than intracerebral injection (15). Depletion of type I IFN receptors in the huCD46 TG mice led to high susceptibility to ED (16–18). These earlier studies, however, were performed before huCD150 was identified as the main receptor for wild-type MV strains (4). No in vivo studies have been attempted using wild-type MV strains and huCD46/huCD150 double TG mice for understanding the mechanisms of wild-type MV infection.

Using huCD150 single TG mice, several reports (12, 13) suggested that wild-type MV strains infect cells that constitutively express huCD150 but fail to induce systemic infection. huCD150 is inducible in human T cells and is up-regulated in myeloid dendritic cells (mDCs) and B cells in response to activation signaling from TLR (19–21). Thus, TG construct with just *lck* or CD11c

*Department of Immunology, Osaka Medical Center for Cancer and Cardiovascular Diseases, Osaka, Japan; †Department of Microbiology and Immunology, Graduate School of Medicine, Hokkaido University, Sapporo, Japan; ‡Genome Information Research Center, Osaka University, Suita, Osaka, Japan; §Department of Virology, Osaka City University Medical School, Osaka, Japan; and ¶Department of Immunology, Graduate School of Medicine and Faculty of Medicine, University of Tokyo, Tokyo, Japan

Received for publication February 4, 2005. Accepted for publication June 15, 2005.

The costs of publication of this article were defrayed in part by the payment of page charges. This article must therefore be hereby marked *advertisement* in accordance with 18 U.S.C. Section 1734 solely to indicate this fact.

[1] This work was supported in part by the Core Research for Evolutional Science and Technology (CREST), Japan Science and Technology Agency, by grants-in-aid from the Ministry of Education, Science, and Culture (Specified Project for Advanced Research), by the Ministry of Health and Welfare of Japan, the Naito Memorial Foundation (to M.M.), and by the Grant 11444 for graduate students from the Ministry of Education, Science, and Culture (to N.I.).

[2] M.S. and N.I. equally contributed to this work.

[3] Address correspondence and reprint requests to Dr. Tsukasa Seya, Department of Microbiology and Immunology, Graduate School of Medicine, Hokkaido University, Kita-ku, Sapporo 060-8637, Japan. E-mail address: seya-tu@med.hokudai.ac.jp

[4] Abbreviations used in this paper: MV, measles virus; BAC, bacterial artificial chromosome; CHO, Chinese hamster ovary; CYT, cytoplasmic tail; DC, dendritic cell; mDC, myeloid DC; pDC, plasmacytoid DC; ED, Edmonston; IC, Ichinose; IFNAR1, type I IFN-$\alpha\beta$ receptor; MALP, macrophage-activating lipopeptide; TG, transgenic; EGFP, enhanced GFP; MOI, multiplicity of infection; $TCID_{50}$, 50% tissue culture infective dose; IRF, IFN regulatory factor; CYT, cytoplasmic tail.

0022-1767/05/$02.00

promoter reported earlier (12, 13) may not be adequate for the study of natural huCD150 distribution, MV entry, and resultant infection via huCD150. Establishment of huCD46/huCD150 double TG mice with human-like distribution profile are necessary for the analysis of wild-type MV spreading and following host immunomodulatory events, particularly measles-mediated immune suppression (22–24).

Therefore, for this study, we generated huCD46/huCD150 double TG mice with or without type I IFN-$\alpha\beta$ receptor (IFNAR1). MV replication and spreading were surveyed by GFP-expressing wild-type Ichinose (IC) strain. In in vivo infection studies, however, neither type of MV was pathogenic to these TG mice irrespective of the route of administration. Analyses of these TG mice suggested that the critical factor in wild-type MV systemic infection appears to depend on the level of type I IFN generated by CD11c-positive dendritic cells (DCs) in this mouse model. In fact, DCs were infected with MV in the huCD150-positive TG mice with no IFNAR1. In this study, we first report that huCD46/huCD150 double TG mice are sensitive to wild-type MV once MV-infected mDCs are supplemented. Thus, infected mDCs facilitate establishing systemic MV infection in the TG mice. These double TG mice allow us to analyze immunomodulatory function of the MV receptors during MV infection (25, 26). The double TG mice with human-like huCD46/huCD150 expression profiles may be a better model for wild-type MV infection compared with huCD150 constitutively expressing mice.

Materials and Methods

Cell culture and reagents

Vero, Vero/huCD150 (a signaling lymphocyte activation molecule (SLAM)), which are Vero cells with stable expression of huCD150 obtained by transfection of huCD150/pCXN2 and antibiotic selection, HEK293, and 293-3-46 cells, kindly provided by M. A. Billeter (Institute of Molecular Biology, University of Zurich, Zurich, Switzerland) were maintained in DMEM supplemented with 10% heat-inactivated FCS and antibiotics. B95a cells were maintained in RPMI 1640 supplemented with 5% heat-inactivated FCS (JRH Biosciences) and antibiotics. Polymyxin B, LPS from *Escherichia coli* serotype O111:B4 was from Sigma-Aldrich. The mycoplasma lipopeptide macrophage-activating lipopeptide (MALP)-2 was prepared as described (27). MALP-2 was treated with polymyxin B (10 μg/ml) for 1 h at 37°C before stimulation of cells (27). Usually, 100 ng/ml LPS and 100 nM MALP-2 were used in mDC TLR stimulation. Isotype controls for PE rat IgG2a, PE rat IgG2b, PE mouse IgG1, PE or FITC golden syrian hamster IgG, FITC mouse IgG1, and FITC mouse IgG2a, and mAbs for PE anti-mouse CD8a, PE anti-mouse CD4, PE anti-mouse CD3e, PE anti-mouse CD19, PE anti-human CD3e, PE anti-human CD4, PE anti-human CD8a, PE anti-human CD19, and FITC anti-huCD150 were obtained from eBioscience. FITC or PE anti-mouse CD11c mAb was obtained from BD Pharmingen. FITC anti-huCD46 (MCP) mAb was obtained from Ancell. HRP-conjugated goat anti-rabbit Igs were obtained from American Qualex. Rabbit polyclonal bodies against huCD150 or huCD46 were produced in our laboratory.

TG method

Spermatozoa were dispersed from epididymis of 12-wk-old mature B6D2F$_1$ male mice in 400 μl of TYH medium diluted to 1 × 10^7/ml and frozen in liquid nitrogen immediately. The bacterial artificial chromosome (BAC) DNA carrying huCD46 or huCD150 was purchased from Incyte Genomics, and purified by using Large-Construct kit (Qiagen) according to the manufacturer's instructions. Each BAC DNA (5 μg/ml in TE buffer) was added to the thawed sperm. The mixtures were incubated for 5 min at room temperature, and mixed with one-tenth volume of 12% PVP-HCZB (polyvinyl-pyrrolidone-HEPES-Chatot, Ziamok, and Barister medium). The metaphase II oocytes for microinjection from B6D2F$_1$ female mice were prepared as previously described (28). These oocytes were maintained in kSOM (potassium simplex optimized medium) under mineral oil equilibrated in 5% (v/v) CO_2 in air at 37°C until use.

Generation of huCD46 and huCD150 TG mice

The huCD46 and huCD150 TG mice were produced by using the intracytoplasmic sperm injection transgene method (29). TG mice were made in accordance of the guidelines of the Animal Care and Use Committee of Osaka University. For microinjection, sperm heads were aspirated into a pipette attached to a piezoelectric pipette-driving unit and a sperm head was injected into each oocyte as previously described (28). After injection, the eggs were incubated in kSOM to the 2-cell stage, and were transferred to ICR pseudopregnant females. Among pups born, the huCD46 and huCD150 TG mice were detected by genomic PCR using huCD46- and huCD150-specific primers. The PCR primers used were as follows: 5′-AAAGGGCAAATTACCTTAGGGGTG-3′ and 5′-AGCACTTCGACC TAAAAATAGAGAT-3′ for huCD46 and 5′-GTGATACAGGAAGCG GGTTCAGG-3′, and 5′-GATACGCTGATTCCTGGCAGCTAAC-3′ for huCD150.

Southern blotting was performed with PCR products from human genome using those primers and with DIG High Prime DNA Labeling and Detection starter kit II (Roche Applied Science).

The IFNAR1$^{-/-}$ mouse (30) was obtained from The Jackson Laboratory. All mice were backcrossed at least six times to be a C57/BL6J background.

Western blotting

Various tissues from huCD46 and huCD150 TG mice were homogenized by a Potter-type homogenizer in 1% (v/v) Triton X-100, PBS, 1 mM PMSF, 10 mM benzamidine, 1 μg/ml pepstatin, and 1 μg/ml lepeptin. The extracts were centrifuged at 15,000 × g, and protein was estimated by Bio-Rad color reagent. A total of 20 μg of protein was subjected to SDS-PAGE under nonreducing conditions and transblotted onto nylon membranes. The membranes were incubated with anti-huCD46 polyclonal Ab or anti-huCD150 polyclonal Ab for 2 h, washed with PBS containing 0.5% Tween 20 three times and incubated with HRP-conjugated goat anti-rabbit Igs for 1 h at 37°C. Following second incubation, the membranes were washed three times with PBS-Tween 20 and proteins were detected with an ECL chemiluminescence kit (Amersham Biosciences).

Plasmid construction and rescue of recombinant viruses

For the preparation of wild-type MV IC-B strain (31, 32) expressing enhanced GFP (EGFP), we constructed p(+)MV323/GFP. Fragment 1, which has *Bss*HII site T7 promoter leader sequence with *Eco*RI site, was amplified by PCR with p(+)MV323/GFP as template using forward primer 5′-AGTCCGCGGGAgcgcgcGTAATACGACTCACTA-3′ (gcgcgc is *Bss*HII site and underline is T7 promoter), and reverse primer 5′-CG gaattcTCCCTAATCCTGCTCTTGTCCC-3′ (gaattc is *Eco*RI site and underline is a part of 5′ noncoding region of the N gene). Fragment 2, which has *Not*I site, the N gene terminator gene junction front half of the N gene with *Hin*dIII site, was amplified by PCR using p(+)MV323/GFP as template with forward primer 5′-CTgcggccgcATTGTTATAAAAAACTTAGG ATTCAAGATCCTATTA-3′ (gcggccgc is *Not*I site and underline is the N gene terminator, gene junction, and the N gene initiator) and reverse primer CCCaagcttCCTCTCGCACCTAGTCTAGAAGAT-3′ (aagctt is *Hin*dIII site and underline is a part of N gene coding region). The fragment 1 was digested with *Bss*HII and *Eco*RI, fragment 2 was digested with *Not*I and *Hin*dIII, and the EGFP gene was cut from pEGFP-N1 plasmid (Clontech Laboratories) with *Eco*RI and *Not*I. These three DNA fragments were ligated and the chimeric plasmid clone containing 5′ *Bss*HII site, T7 promoter, leader initiation signal (the 5′ region of the N gene) EGFP gene, and junction (a termination sequence of the 3′ region of the N gene/CTT sequence (the 5′ region of the N gene containing an initiation sequence), which have *Esp*I site) 3′ sequences, was generated. The accuracy of the fragment was confirmed by sequencing. The insert and p(+)MV323 were digested with *Bss*HII and *Esp*I, and the fragment containing an EGFP gene was inserted into p(+)MV323.

Recovery of infectious MV was performed as previously described (33, 34). MV323, MV323/GFP, and MV2A (ED strain) were recovered from p(+)MV323, p(+)MV323/GFP, and p(+)MV2A, respectively.

Immunofluorescence staining and confocal microscopy

Mock- or MV323GFP-infected mouse splenocytes were stained with PE rat IgG2a isotype control, PE rat IgG2b isotype control, PE golden syrian hamster IgG isotype control, PE anti-mouse CD8a mAb, PE anti-mouse CD4 mAb, PE anti-mouse CD3e mAb or PE anti-mouse CD19 mAb for 30 min at 4°C in FACS buffer. After washing, the stained cells were fixed in 0.5% formaldehyde in PBS and visualized at a magnification ×60 under a FLUOVIEW (Olympus). Images were captured using the attached computer FLUOVIEW software.

FACS cytometric analysis of cell surface Ags

FACS methods were previously described (35). Briefly, cells were suspended in PBS containing 0.1% sodium azide and 1% BSA (FACS buffer) and incubated for 30 min at 4°C with FITC-labeled mAbs and PE-labeled mAbs. Cells were washed and fluorescence intensity was measured by FACS.

Preparation of MV strains and in vitro MV infection analysis

Recovered viruses, MV2A (ED strain), MV323 (IC-B strain), and MV323GFP (IC-B strain containing EGFP gene), were passaged in B95a cells and titrated on Vero/SLAM cells. Low-passaged viruses were used in this experiment. The receptor usage of the strains was confirmed on Chinese hamster ovary (CHO), CHO/huCD46, or CHO/huCD150 cells (5). For in vitro viral infection assay, single cell suspensions of spleen from TG or non-TG littermates were obtained by passage thought sterile mesh. After removing erythrocytes using Lympholyte-M (Cedarlane Laboratories), purified cells were cultured in RPMI 1640 supplemented with 10% heat-inactivated FCS, 10 mM HEPES, 1 mM sodium pyruvate, 0.1 mM nonessential amino acids, 0.05 mM 2-ME, 50 U/ml mouse IL-2, 20 ng/ml PMA, and 1 μg/ml ionomycin for 24 h. FACS analysis was performed 48 h after infection.

Preparation of DCs

Mouse bone marrow-derived mDCs were prepared by the modified technique (36, 37) of earlier reported method (38). Briefly, 0.5–1 $\times$ 10^6 bone marrow cells/2 ml/well in RPMI 1640 supplemented with 10% heat-inactivated FCS, 10 mM HEPES, 1 mM sodium pyruvate, 0.1 mM nonessential amino acids, and 0.05 mM 2-ME were cultured overnight in 24-well plates. Nonadherent cells were harvested, resuspended in the same medium supplemented with 10 μg/ml mouse GM-CSF, and cultured in the mouse GM-CSF-containing medium. On day 3, adherent cells were cultured in fresh medium with 10 μg/ml mouse GM-CSF. On day 6, nonadherent cells and loosely adherent cells were harvested and used for experiments as immature DCs (38). Immature DCs were resuspended and cultured in fresh RPMI 1640 medium with 10 μg/ml mouse GM-CSF. Cellular RNA was estimated 24 h postinfection.

Human PBMC were isolated from buffy coat of normal healthy donors by methylcellulose sedimentation followed by standard density gradient centrifugation with Ficoll-Hypaque (Amersham Biosciences) (27). For human immature DC preparation, $CD14^+$ monocytes were obtained from human PBMC by using MACS system (Miltenyi Biotec) with anti-human CD14 mAb-conjugated microbeads and kept in RPMI 1640 (Invitrogen Life Technologies) containing 10% FCS, 500 IU/ml human GM-CSF, 100 IU/ml human IL-4 (PeproTech), and antibiotics for 6 days. Morphological changes were examined by phase contrast microscopy (Olympus IX-70).

Assay of in vivo MV infection

Newborn 2-day-old, 1-wk-old, or 6- to 10-wk-old TG or non-TG mice were injected i.p., i.v., intranasally, and s.c. with MV323GFP at a dose of 5×10^4 50% tissue culture infective doses ($TCID_{50}$). Mice were sacrificed 2–4 days after inoculation, and each tissue was collected and fixed with 4% paraformaldehyde in PBS overnight at 4°C. Tissues were embedded in Tissue-Tek OCT compound (Miles) and quickly frozen in liquid nitrogen. Serial frozen sections (10-μm thick) were cut with the cryostat (Leica) and were analyzed by confocal microscopy.

In vitro splenocytes proliferation assay

Splenocytes (1×10^5/100 μl/well in 96-well plate) freshly isolated from each TG mouse were stimulated with 20 ng/ml PMA and 1 μg/ml ionomycin in the presence of 50 U/ml mouse IL-2, and infected by MV323. Twenty-four hours later the cells were labeled for 16 h with [^{3}H]thymidine (1 mCi/ml). The incorporated counts were determined using a beta-plate reader in triplicate.

RT-PCR and quantitative PCR

Mouse mDCs or splenocytes were treated with trypsin and collected by centrifugation at 1500 $\times$ *g* for 10 min. Total RNA was extracted with RNeasy mini kit (Qiagen). A total of 2 μg of total RNA was incubated at 70°C for 5 min, kept on ice for 2 min, and reverse transcription was performed with Moloney murine leukemia virus-reverse transcriptase (Promega) at 37°C for 90 min followed by PCR or quantitative PCR. Following primers were used for PCR: α-IFN forward, 5′-AGTGATGAGCTAC TGGTCAAC-3′; reverse, 5′-TGATGCTGTGGAAGTATATCCTC-3′; β-IFN forward, 5′-TCCAGCTCCAAGAAAGGACG-3′; reverse, 5′-GCATCTTCTCCGTCATCTCC-3′; γ-IFN forward, 5′-AGACAGAAGT TCTGGGCTTCTC-3′; reverse, 5′-GGGTTGTTGACCTCAAACTTGG-3′; MV-H forward, 5′-CCCTTATCAACGGATGATCC-3′; reverse, 5′-GT GATCAATGGCCCGAATCC-3′; MV-N forward, 5′-AAGGTCAGTTC CACATT-3′; reverse, 5′-GAAGATCTCTGTCATTG-3′; IL-12 p40 forward, 5′-GAGTCATAGGCTCTGGAAAGACC-3′; reverse, 5′-AGTT GGGCAGGTGACATCC-3′; IL-10 forward, 5′-GGTTGCCAAGCCT TATCGGA-3′; reverse, 5′-ACCTGCTCCACTGCCTTGCT-3′; β-actin forward, 5′-ATCATGTTTGAGACCTTCAACACC-3′; reverse, 5′-GAT GTCACGCACGATTTCCC-3′; and HPRT (hypoxanthine phosphoribosyltransferase) forward, 5′-GTTGGATACAGGCCAGACTTTGTTG-3′, reverse, 5′-GAAGGGTAGGCTGGCCTATAGGCT-3′.

Reaction for quantitative PCR was done with iQ SYBER Green Supermix, and amplified PCR products were measured by iCycler iQ Real-Time PCR analyzing system (Bio-Rad). Normalized value for each mRNA expression was calculated as relative quantity of mRNA divided by the relative quantity of mouse hypoxanthine phosphoribosyltransferase.

Determination of human IFN-β level

Culture media were centrifuged to remove cell debris and supernatants were stored at −80°C until the assay. The level of secreted human IFN-β in the culture medium was determined with an ELISA kit (FUJIREBIO) for human IFN-β according to the manufacturer's protocol.

Results

Human-like expression of huCD46 or huCD150 in TG mice

Ubiquitous expression of huCD46 was not obtained in TG mice that were previously generated with huCD46 cDNA (39). A number of splicing variants in huCD46, which appeared in an organ-specific manner (40), participated in differential cell-mediated immune response (26). To generate the natural expression profile of huCD46 and its isoforms, we transferred the 194-kb BAC DNA carrying the huCD46 gene into mouse embryo and obtained TG mice with human-like CD46 expression pattern. Similarly, huCD150 TG mice were generated by transferring the huCD150 BAC DNA (185 kb) into mouse embryo. These mice have a human-like CD150 expression profile, which is inducible in T cells and up-regulated in mDCs and B cells. We examined the expression profiles of huCD46 and huCD150 in various organs of each line of our TG mice by SDS-PAGE and Western blotting (Fig. 1*A*). In huCD46 TG mice, huCD46 was ubiquitously expressed with the size variation of isoforms in an organ-specific fashion similar to human (41, 42). The brain of these mice notably expressed a low molecular mass moiety of huCD46 in the TG mice similar to human form. In addition, similar to human, huCD150 appeared in a tissue-specific manner in the thymus and spleen in huCD150 TG mice. In non-TG mice, no signals of huCD46 or huCD150 were detected in Western blots, suggesting no cross-reaction of the Abs with the mouse counterparts.

Cell populations expressing huCD46 or huCD150 in TG mice

We next analyzed cells from spleens of huCD46 TG, huCD150 TG, or non-TG mice by FACS analysis (Fig. 1*B*). In huCD46 TG mice, huCD46 was expressed on the surface of both CD3- or CD19-positive splenocytes. In huCD150 TG mice, huCD150 was expressed on CD19-positive cell surface, but minimal expression occurred on CD3-positive cells. Neither CD4 nor CD8 T cells expressed huCD150 (data not shown). Under similar FACS conditions, human PBMC ubiquitously expressed CD46 and partly expressed CD150 (Fig. 1*B*, *right*). When splenocytes from huCD150 TG mice were stimulated with PHA (data not shown) or PMA, ionomycin, and murine IL-2 (Fig. 1*C*, *left*), FACS profiles of the lymphocyte populations were altered. In addition, the levels of huCD150 in $CD4^+$ and $CD8^+$ T cell and $CD19^+$ B cell populations were up-regulated (Fig. 1*C*). Similar results were obtained with human PBMC when the cells were similarly stimulated (Fig. 1*C*, *right*). Neither huCD46 nor huCD150 was expressed in cells from non-TG mice as expected (see Fig. 5, *B* and *C*, labeled as

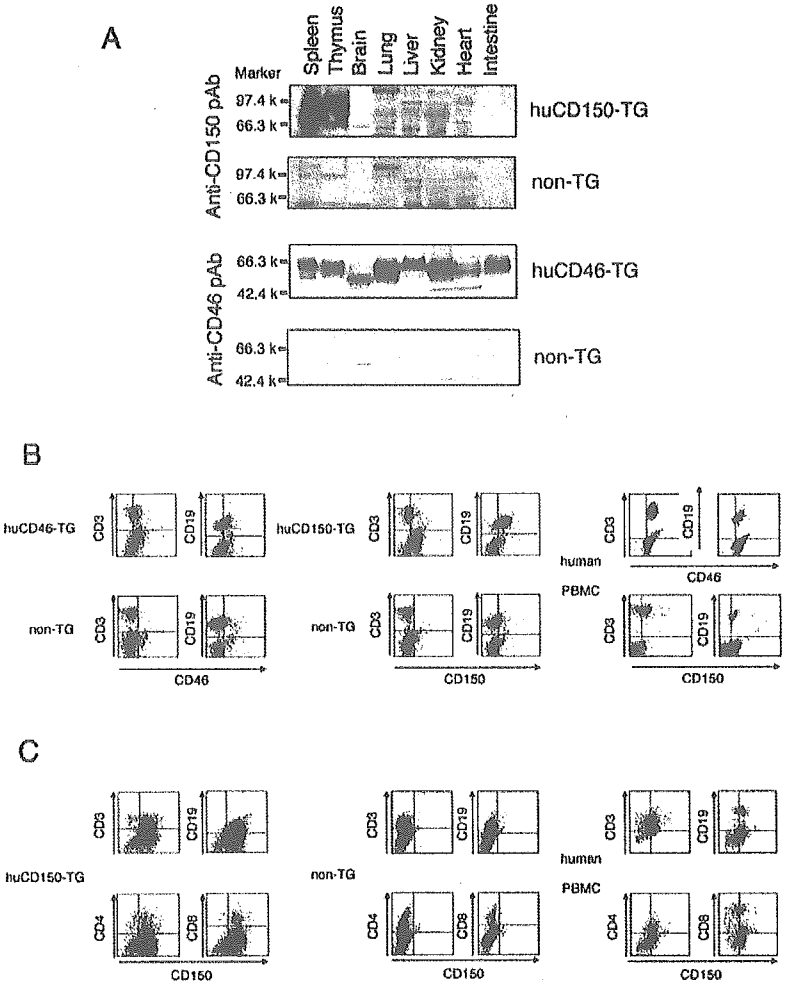

FIGURE 1. Generation of huCD46 and huCD150 TG mice. A, Western blot analysis of huCD46 and huCD150 in TG mice. Various tissues from huCD46 TG and huCD150 TG mice were homogenized and the extracts were separated by SDS-PAGE under nonreducing conditions and transblotted onto a nylon membrane. The huCD46 and huCD150 were then visualized with anti-human CD46 polyclonal Ab and anti-human CD150 polyclonal Ab, respectively, produced in our laboratory (64). *B* and *C*, FACS analysis for detection of huCD46 and huCD150 in mouse spleen cell populations and human PBMC. Freshly isolated splenocytes from the huCD46 and huCD150 TG mice or human PBMC were stained with FITC-labeled anti-human CD46 or CD150 mAb, and PE-labeled mCD3, mCD4, mCD8, or mCD19 mAb before (*B*) or after (*C*) stimulation with PMA and ionomycin.

"non-TG"). These results show that huCD150-inducible TG mice were established, which may suit the study for susceptibility of cell species to MV strains.

We then generated huCD46/huCD150 double TG mice by mating both TG lines (Fig. 2*A*). Gene analysis showed that the littermates of huCD46/huCD150 TG, huCD46 TG, huCD150 TG, and non-TG mice followed Mendel's laws of inheritance (Fig. 2*A*), suggesting that huCD46/huCD150 transgene does not bring about any lethal defect. The presence of huCD46 and huCD150 genes in litters was monitored by PCR (data not shown) and confirmed by Southern blot analysis (Fig. 2*B*). Expression profiles of huCD46 and huCD150 in each litter were also confirmed by Western blot and FACS analysis (data not shown).

Preparation of EGFP-labeled MV

To monitor MV infection, we generated EGFP-expressing recombinant MV (IC323GFP) based on the wild-type IC strain. Plasmid containing full-length cDNA of the IC strain and the EGFP gene was constructed as shown in Fig. 3*A*. GFP expression reflects viral replication in this construct. The rescued MV323GFP showed almost the same growth kinetics as the parental recombinant MV323. Its receptor usage was confirmed with CHO cells expressing huCD46 or huCD150 (Fig. 3*B*). MV2A (ED strain) rescued from p(+)MV2A, was used as the laboratory-adapted strain. When infected with MV2A, both CHO/huCD46 and CHO/huCD150 cells produced the typical syncytia, whereas MV323 infected CHO/huCD150 cells but not CHO/huCD46 cells (data not shown). MV323GFP also infected CHO/huCD150 cells to form syncytia exhibiting green autofluorescence, but did not form any syncytium in CHO/huCD46 and intact CHO cells.

In vitro analysis of MV infection of splenocytes from TG mice

To examine in vitro MV infection, the splenocytes were isolated from each TG mouse and infected with MV323GFP at a multiplicity of infection (MOI) of 0.25 (Fig. 4*A*). When prestimulated with PMA and ionomycin, some splenocytes from the double TG or huCD150 TG mice were positive in GFP, a marker for infection. The stimulation was essential for MV permissiveness as reported before (14). However, under any infectious conditions the splenocytes from huCD46 TG and non-TG mice were GFP-negative. The results were confirmed to be reproducible by semiquantitative FACS analysis (Fig. 4*A*). In contrast, MV323GFP infected human PBMC even at low MOI of inoculation (Fig. 4*A*, *bottom panels*). Human PBMC appear to be more susceptible to MV323GFP than the splenocytes of the double TG and huCD150 TG mice.

To examine which populations of splenocytes of huCD46/huCD150 TG or huCD150 TG mice were infected with MV323GFP, we segregated them with PE-conjugated anti-mouse CD3, CD4, CD8, CD11c, or CD19 mAb and analyzed them by FACS and confocal microscopy (Fig. 4, *B* and *C*). MV323GFP inoculation rendered the CD3-, CD4-, CD8-, and CD19-positive cells green. But CD11c-positive cells barely turned green even at